

## Early life exposure to broccoli sprouts confers stronger protection against enterocolitis development in an immunological mouse model of inflammatory bowel disease.

Lola Holcomb<sup>1§</sup>, Johanna Holman<sup>2§</sup>, Molly Hurd<sup>3</sup>, Brigitte Lavoie<sup>3</sup>, Louisa Colucci<sup>4</sup>, Benjamin Hunt<sup>5</sup>, Timothy Hunt<sup>5</sup>, Gary M. Mawe<sup>3</sup>, Peter L. Moses<sup>3,6</sup>, Emma Perry<sup>7</sup>, Allesandra Stratigakis<sup>8</sup>, Tao Zhang<sup>8</sup>, Grace Chen<sup>9</sup>, Suzanne L. Ishaq<sup>1\*</sup>, Yanyan Li<sup>1\*</sup>

<sup>1</sup> Graduate School of Biomedical Sciences and Engineering, University of Maine, Orono, Maine, USA 04469

<sup>2</sup> School of Food and Agriculture, University of Maine, Orono, Maine, USA 04469

<sup>3</sup> Larner College of Medicine, University of Vermont, Burlington, Vermont, USA 05401

<sup>4</sup> Department of Biology, Husson University, Bangor, Maine, USA 04401

<sup>5</sup> Department of Biology, University of Maine, Orono, Maine, USA 04469

<sup>6</sup> Finch Therapeutics, Somerville, Massachusetts, USA 02143

<sup>7</sup> Electron Microscopy Laboratory, University of Maine, Orono, Maine, USA 04469

<sup>8</sup> School of Pharmacy and Pharmaceutical Sciences, SUNY Binghamton University, Johnson City, New York, USA 13790

<sup>9</sup> Department of Internal Medicine, University of Michigan Medical School, Ann Arbor, Michigan, USA 48109

§ these authors contributed equally.

### \*Corresponding authors:

Suzanne L. Ishaq, University of Maine, School of Food and Agriculture, Orono, ME 04469, [sue.ishaq@maine.edu](mailto:sue.ishaq@maine.edu), 1-207-581-2770

Yanyan Li, University of Maine, School of Food and Agriculture, Orono, ME 04469, [yanyan.li@maine.edu](mailto:yanyan.li@maine.edu), 1-207-581-3134

**Keywords:** Crohn's Disease, cruciferous vegetables, sulforaphane, glucoraphanin, gut microbiota, dietary bioactives, 16S rDNA, interleukin-10 knockout

### Abstract

Inflammatory Bowel Diseases (IBD) are chronic conditions characterized by inflammation of the gastrointestinal tract that heavily burden daily life, result in surgery or other complications, and disrupt the gut microbiome. How IBD influences gut microbial ecology, especially biogeographic patterns of microbial location, and how the gut microbiota can use diet components and microbial metabolites to mediate disease, are still poorly understood. Many studies on diet and IBD in mice use a chemically induced ulcerative colitis model, despite the availability of an immune-modulated Crohn's Disease model. Interleukin-10-knockout (IL-10-ko) mice on a

C57BL/6 background, beginning at age 4 or 7 weeks, were fed either a control diet or one containing 10% (w/w) raw broccoli sprouts which was high in the sprout-sourced anti-inflammatory sulforaphane. Diets began 7 days prior to inoculation with *Helicobacter hepaticus*, which triggers Crohn's-like symptoms in these immune-impaired mice, and ran for two additional weeks. Key findings of this study suggest that the broccoli sprout diet increases sulforaphane concentration in plasma; decreases weight stagnation, fecal blood, and diarrhea associated with enterocolitis; and increases microbiota richness in the gut, especially in younger mice. Sprout diets resulted in some anatomically specific bacterial communities in younger mice, and reduced the prevalence and abundance of potentially pathogenic or otherwise-commensal bacteria which trigger inflammation in the IL-10 deficient mouse, for example, *Escherichia coli* and *Helicobacter*. Overall, the IL-10-ko mouse model is responsive to a raw broccoli sprout diet and represents an opportunity for more diet-host-microbiome research.

## Importance

A diet containing 10% raw broccoli sprouts increased the plasma concentration of the anti-inflammatory compound sulforaphane, and may be protective against negative disease characteristics of *Helicobacter*-induced enterocolitis in interleukin-10 knockout mice, including weight loss or stagnation, fecal blood, and diarrhea. Younger mice responded more strongly to the diet intervention, and resulted in increased gut bacterial community richness and bacterial community similarity by diet treatment and some anatomical locations in the gut, even in mice with adverse reactions to gut microbiota and a relatively short time in which they had been able to recruit them. To our knowledge, IL-10-ko mice have not previously been used to investigate the interactions of host, microbiota, and broccoli, broccoli sprouts, or broccoli bioactives in resolving symptoms of CD.

## Introduction

Inflammatory Bowel Diseases (IBD) affect more than 6 million people globally, with more than 25% of cases reported in the United States (1). The varied combination of symptoms, the intensity of presentation, and their multifactorial origin make symptoms difficult to manage, and leads to significant detriment to quality of life. Crohn's Disease (CD) is one of the primary immune-disordered presentations of IBD which typically presents during late adolescence and early adulthood (2), has strongly associated genetic (3) and environmental (4, 5) factors, and involves a loss of function of the innate immune system which disrupts host-microbial interactions in the gastrointestinal tract (6). CD treatments attempt to alleviate inflammation as a method of reducing various symptoms, and to return patients to as close to homeostasis as possible, although single-strategy treatments can yield mixed results (7). Diet can play an important, economical, and accessible role in the prevention and/or management of IBD as a source of anti-inflammatory metabolites (8, 9), and broadly as a tool for influencing the robustness of gut microbiomes (10–12). How IBD affects gut microbial ecology (13, 14), how gut microbiota mediate disease (15) or response to diet (16, 17), and how dietary components and microbial metabolites improve symptoms are still poorly understood (18, 19). Moreover, the delicate health status in CD patients requires a thorough understanding of host-microbe-diet interactions before suggesting therapeutic strategies.

Diets high in cruciferous vegetables, such as broccoli and broccoli sprouts, have particularly been associated with reducing inflammation and cancer risk in the gut (9, 20), in part because of the concentration of sulfur-containing glucosinolates which can be metabolized to bioactive compounds by broccoli- or microbially-sourced enzymes. Isothiocyanates, derived from glucosinolates, have been identified as bioactive candidates for inflammation reduction, including in IBD (9). Specifically, sulforaphane (SFN), the most well-studied isothiocyanate, inhibits the immune factor NF- $\kappa$ B and downregulates multiple inflammatory signaling pathways (9). Broccoli sprouts, or the purified SFN or precursor compounds, protect against chemical-induced ulcerative

colitis in mice (20, 21), but the applicability of previous diet research to CD has been hampered by the use of mouse models which lack the complex immune-dysfunction component of CD (22, 23). Medical professionals will need a clear understanding of how the immune system in CD patients will react to the microbiota changes induced by diet (18, 24), and especially the inclusion of a sulfur-rich diet which complicates host-microbe interactions in the gut (25), as CD patients are historically been advised to avoid cruciferous vegetables (24).

Inflammation in CD is relapsing, occurs throughout the gastrointestinal tract, and results in several breakdowns of the innate immune system to allow microbial translocation from gut to other tissues. This includes decreased expression of the MUC1 gene, leading to reduced coverage of mucin in the ileum (26), reduced efficacy of tight junction proteins (27), and a loss of absorption of bile salts in the ileum which causes damage to the colon. Acute, non-pathological inflammation is a normal component of the innate immune response. This response is reportedly weak in CD patients who have low neutrophil counts in response to infection (6), in whom uncleared infection and infiltration of fecal material through the mucosal lining of the gastrointestinal tract drives dysregulation of the adaptive immune response and results in chronic inflammation (6, 28). The adaptive immune response in CD primarily involves excessive recruitment of effector T-cells (Th1 and Th17) by inflammatory cytokines (interleukins -12, -18, and -23) which are upregulated in CD lesions (2, 29, 30). In addition to being chronic and debilitating, the duration of IBD and of inflammation, damage to intestinal walls, and other negative outcomes, are associated with an increased risk of developing gastrointestinal cancers, such as colorectal cancer (31).

The interleukin 10 (-/-) knockout mouse model is commonly used to study inflammation in CD (32). Interleukins (IL) are signaling proteins that aid in immune function by reducing inflammation and counterbalancing the immune response, thus mediating host-microbial tolerance (33). IL-10 also stimulates the growth and differentiation of numerous cell types, suppresses macrophage activation, inhibits inflammatory cytokine production, and displays

multiple mechanisms of control of Th1 cells (34). IL-10, in particular, influences the innate immune response to microorganisms, and a lack of it is involved in the breakdown of host-microbial relations in IBD (35). IL-10 deficient mice (IL-10-ko) are raised in germ-free conditions, and develop chronic enterocolitis upon exposure to microorganisms which act commensally in immune-competent mice, and this response resembles the transmural inflammation of CD, complete with the formation of granulomas, crypt abscess, mucosal hyperplasia, as well as aberrant immune cell response (36, 37). This non-chemical, genetic model is particularly well-suited to studying the immune factors and microbiota of CD (38).

To our knowledge, IL-10-ko mice have not previously been used to investigate the interactions of host, microbiota, and broccoli, broccoli sprouts, or broccoli bioactives in reducing inflammation, modifying the immune response, and supporting gastrointestinal tract microbial systems in CD patients, and the objective of this study was to evaluate IL-10-ko mice as a model for studying the broccoli sprout bioactives. Our initial hypothesis was that a medium-high concentration (10% w/w) of raw broccoli sprouts in the diet, which contains both the glucoraphanin (GLR) precursor and the anti-inflammatory byproduct sulforaphane (SFN), would protect mice from the effects of inflammation triggered by microbial conventionalization, even in the absence of a developed gut microbiota which would perform glucosinolate metabolism. We hypothesized that the sprout diet would alter the gut microbiota, and result in the recruitment of potentially beneficial taxa while reducing the abundance of putative pathogens. It is standard to conventionalize IL-10-ko at approximately 8 weeks of age, after mice are fully weaned (39), to mimic adolescence and typically timing for the onset of symptoms. In conducting two replications of a diet trial with mice beginning at 4-weeks and 7-weeks of age, we observed a previously unreported effect of young age on the effectiveness of the response to broccoli sprout bioactives in resolving the symptoms of enterocolitis.

## Results

### Raw broccoli sprouts alleviated disease characteristics of immune-modulated enterocolitis

The experimental design was structured as a prevention paradigm (Figure 1) in which homozygous interleukin-10 knockout (IL-10-ko) mice were given *ad libitum* either the 5LOD irradiated control diet or the treatment diet consisting of 10% (w/w) raw broccoli sprouts for 7 days to allow them to acclimate, then for a further 16 days during the induction of colitis via microbial colonization and symptom onset. Raw broccoli sprouts contain concentrated amounts of glucoraphanin, some of which is metabolized to sulforaphane by mastication, or in this case, diet preparation, when the broccoli enzyme myrosinase is released from tissues. The control diet contained no GLR or SFN, and the broccoli diet contained on average 4  $\mu\text{g}$  of GLR and 85  $\mu\text{g}$  of SFN.

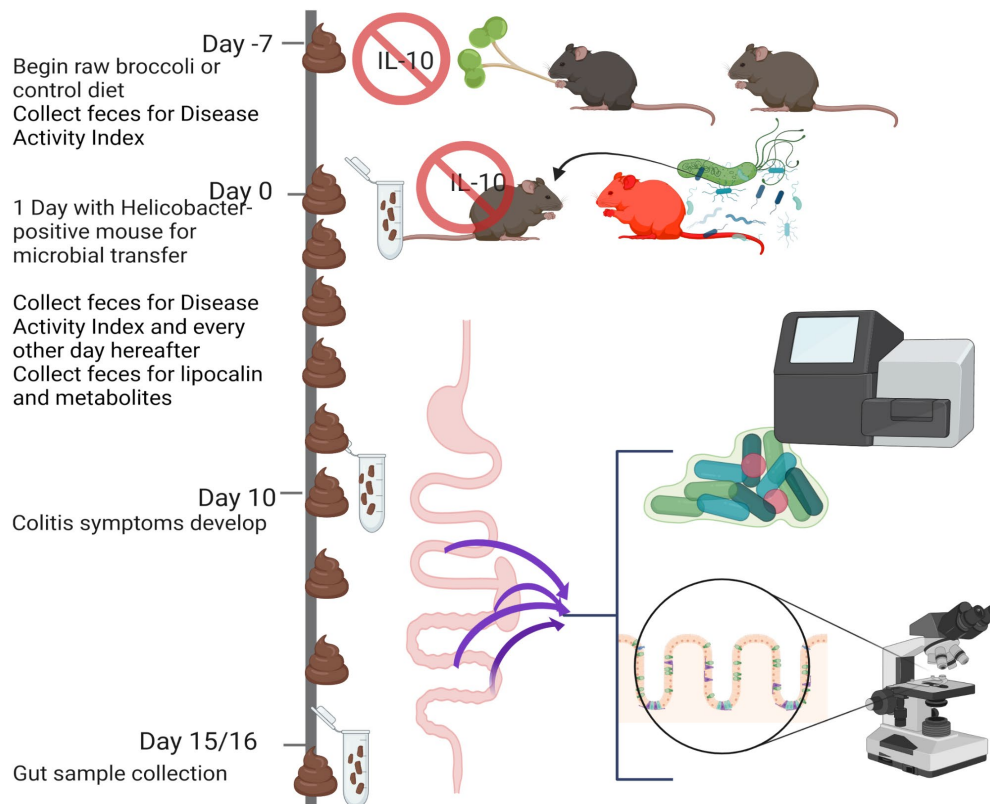


**Figure 1. Experimental design.**

Trial 1 included 9 mice (n = 5 in the treatment group and 4 in the control group) starting at 4 weeks of age, and Trial 2 included 10 mice (n = 5 in the treatment group and 6 in the control group) starting at 7 weeks of age, which is the standard age for IL-10 microbiota trials. The younger mice that were fed the broccoli diet continued to gain weight once enterocolitis was induced compared to their baseline weight, and the younger mice fed the control diet plateaued around 120% of body weight (Figure 2A, ANOVA  $p < 0.05$ ). The older mice had a similar weight stagnation during enterocolitis regardless of diet (Figure 2B). Consumption of the broccoli diet significantly attenuated the development of inflammation in IL-10 KO mice regardless of age group, indicated by lower DAI scores, corresponding to firmer stool and the lack of blood in stool (Figure 2, ANOVA  $p < 0.05$ ).

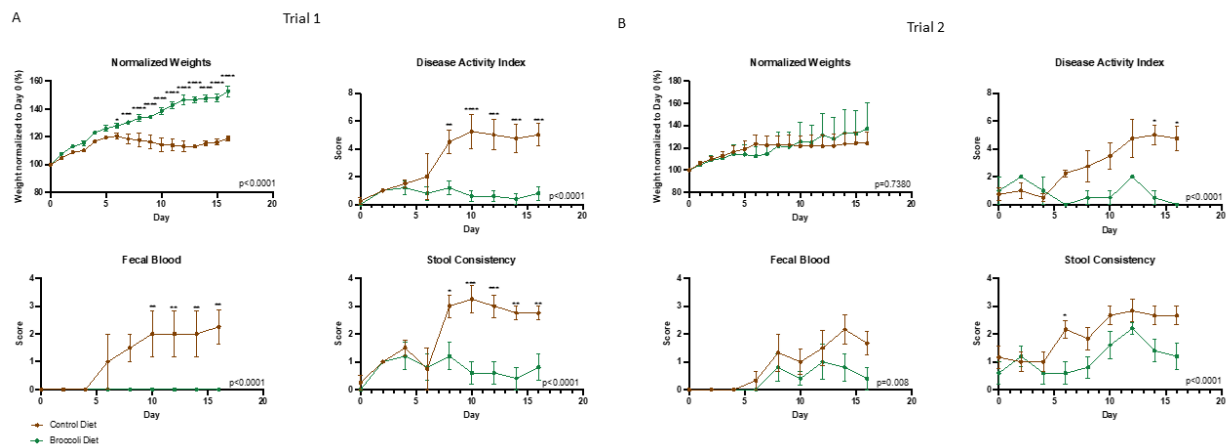


**Figure 2. A one-week pretreatment, and continuation of a diet containing 10% broccoli sprouts significantly attenuated the development of colitis in IL-10-ko mice (broccoli, n=10; control, n=10).** A) IL-10-ko mice used were 4 - 6 weeks old for the duration of the first trial, and B) 7 - 9 weeks old in the second trial. In the IL-10-ko model, animals with colitis tend to continue gaining weight, but more slowly. Thus, the animal's weights were normalized to their weight on the day of microbial exposure. Disease Activity Index scores are compiled from weight loss, fecal blood, and fecal consistency scores. Overall model significance is included on the chart, and single timepoint comparisons significance was designated as  $p < 0.05$ ; \*\* $p < 0.01$ ; \*\*\* $p < 0.001$ ; \*\*\*\* $p < 0.0001$  by two-way ANOVA, and post multiple comparisons by Sidak.

Sulforaphane (SFN) in the gut was absorbed by the mice consuming broccoli sprouts and was found in high concentrations in their plasma, while control mice exhibited no circulating SFN (Figure 3A, ANOVA  $p < 0.05$ ). Fecal lipocalin (LCN2), a neutrophil protein that binds bacterial siderophores, serves as a biomarker for intestinal inflammation (40). Analysis of fecal samples on the day of microbial exposure for conventionalization (D0), appearance of symptoms (D10), and end of the trial (D15/16) revealed a markedly lower LCN2 concentration in the group of mice fed the 10% raw broccoli sprouts diet compared to those fed the control diet at both Day 10 and Day 15/16 (Figure 3B, ANOVA  $p < 0.05$ ).

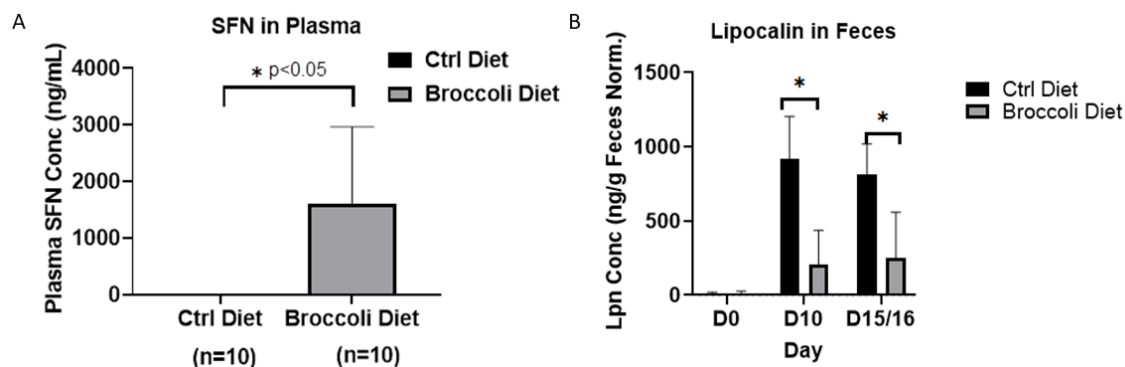


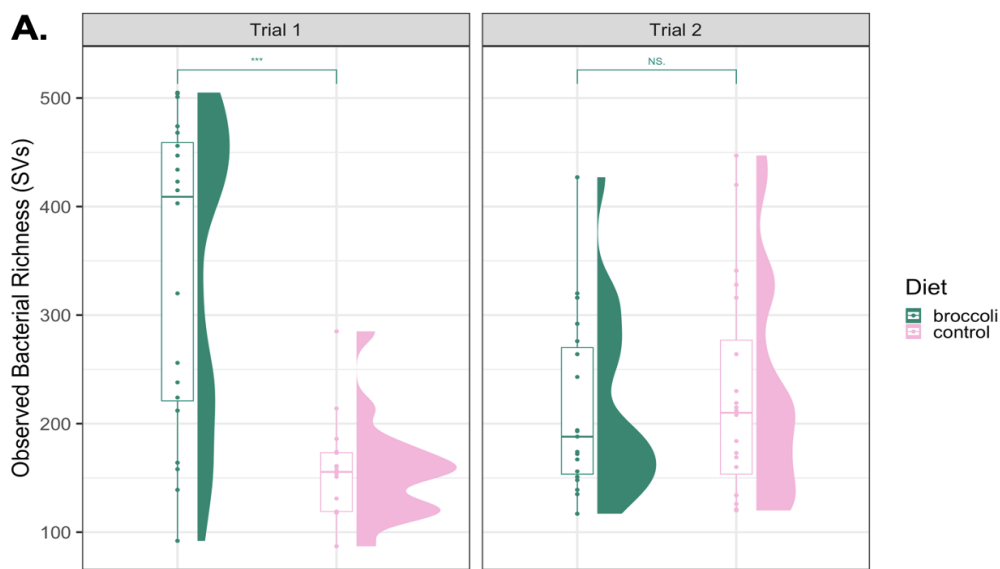
**Figure 3. Levels of (A) plasma sulforaphane and (B) fecal lipocalin measured by ELISA in conventionalized IL-10-ko mice during a diet trial featuring 10% (w/w) raw broccoli sprouts or control diets.** Stool samples were collected from mice (n=10/group) on Days 0 (conventionalization), 10 (onset of symptoms), and 15/16 of experiment for Lipocalin-2 concentration determination. Plasma was collected on Days 15/16 for sulforaphane concentration. Data were similar across both trials and combined. For lipocalin, data was normalized by the weight of feces, and significance set as \*  $p < 0.05$ .

Tissue from the ileum, proximal colon, and distal colon were collected for histological scoring (0 = no signs, and 2 = significant signs) of epithelial damage, architectural changes, infiltration of mononuclear cells into the lamina propria, infiltration of polymorphonuclear cells in the lamina propria or into the epithelium, as well as abscesses, ulcers, erosion, and branched crypts which were scored together (Figure S1). Treatment was not a significant factor in linear models for each of the scoring criteria, even when data were subset into trial 1 or 2, or subset into ileum, proximal colon, and distal colon. The exception to this was infiltration of mononuclear cells

into the lamina propria, which was significantly lower (linear regression model (lm),  $p = 0.02$ ) in the broccoli sprout mice compared to control mice in trial 1.

### Age significantly influenced bacterial community responsiveness to raw broccoli sprouts

Of the three experimental factors analyzed in this study, we report that age is the most significant factor (relative to diet and anatomical location) in driving gut bacterial community richness, membership, and similarity between samples. In trial 1 group, mice that started consuming the raw broccoli sprouts at 4 weeks of age had greater observed bacterial richness by 6 weeks of age than their counterparts fed a control diet (Figure 4A, permANOVA  $p < 0.05$ ). However, mice in trial 2, starting at 7 weeks, showed no significant difference in bacterial richness between the two treatment groups by age 9 weeks (Figure 4B, permANOVA  $p > 0.05$ ). When comparing the effect of diet on bacterial communities within each age group and within each of the four anatomical locations studied, the broccoli sprout diet increased bacterial richness in the cecum and the proximal colon of the younger mice, compared to the younger controls (Figure 4B, Wilcox tests  $p < 0.05$ ). There was no difference between bacterial richness in any gut location in the older mice consuming broccoli sprouts versus the control diet.



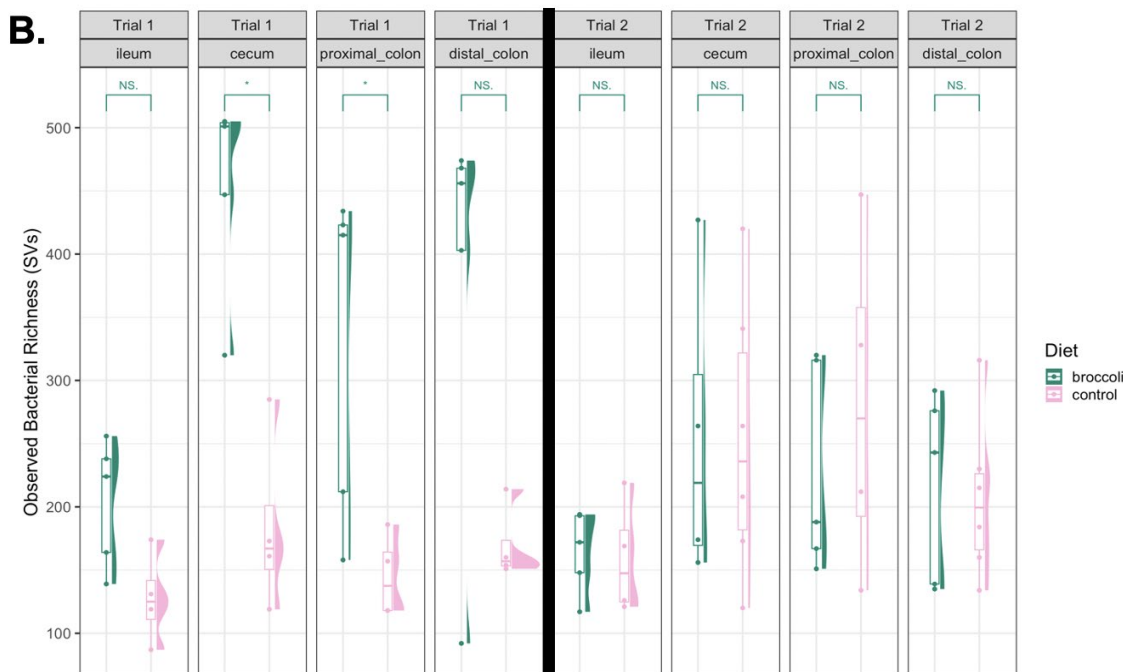


**Figure 4. Observed bacterial richness within the gastrointestinal tracts IL-10-KO mice fed control diets or raw broccoli sprout diets from 4-6 weeks of age (Trial 1) and 7-9 weeks of age (Trial 2).** Panel A shows comparison of broccoli-fed and control mice in Trial 1 and Trial 2 mice across the whole gastrointestinal tract (\*\* $p < 0.001$ ); Panel B shows comparisons of broccoli-fed and control mice in which were 4 - 6 weeks old for the duration of the first trial and 7 - 9 weeks old in the second trial, in each anatomical location scraping site (\* $p < 0.05$ ). Graphics made using phyloseq and ggplot2 packages in R. Significance added by Wilcox tests from ggsignif package in R.

When comparing bacterial community similarity between samples, age was again the strongest explanatory factor in both unweighted (bacterial taxa presence/absence, Figures S2, S3) and weighted (bacterial taxa presence and abundance, Figure 5, 6) metrics. Within the trial 1 group, broccoli-fed samples clustered separately from control samples (Figure 5; Table 1, permANOVA  $p < 0.001$ ), showing a significant difference in microbiota beta diversity between the two dietary treatment groups. This was in part due to significant taxonomic dissimilarity between the two diets in the cecum and from the distal colon between the two diet groups (Figure 6, Table 1), and differences in beta diversity within the proximal colon were nearly statistically significant.

Like the trial 1, dietary treatment was the most significant driver of bacterial community similarity in the older trial 2 mice, but to a lesser extent (Figure 5; Table 1, permANOVA: lower F values,  $p < 0.03$ ). Overall, anatomical location was a significant factor, however; within each of

the four anatomical locations studied, there was no significant diet effect shown within the older trial 2 group ( $p > 0.05$ ). The bacterial taxa which drove the differences between age, diet, and anatomical treatment were primarily different SVs identified to the Muribaculaceae family (Figure S4), a taxon of common mouse commensals. SVs in the Muribaculaceae made up much of the core microbiota specific to each group, as well as several SVs identified to Lachnospiraceae, *Bacteroidetes*, *Helicobacter*, and others (Figure S5).

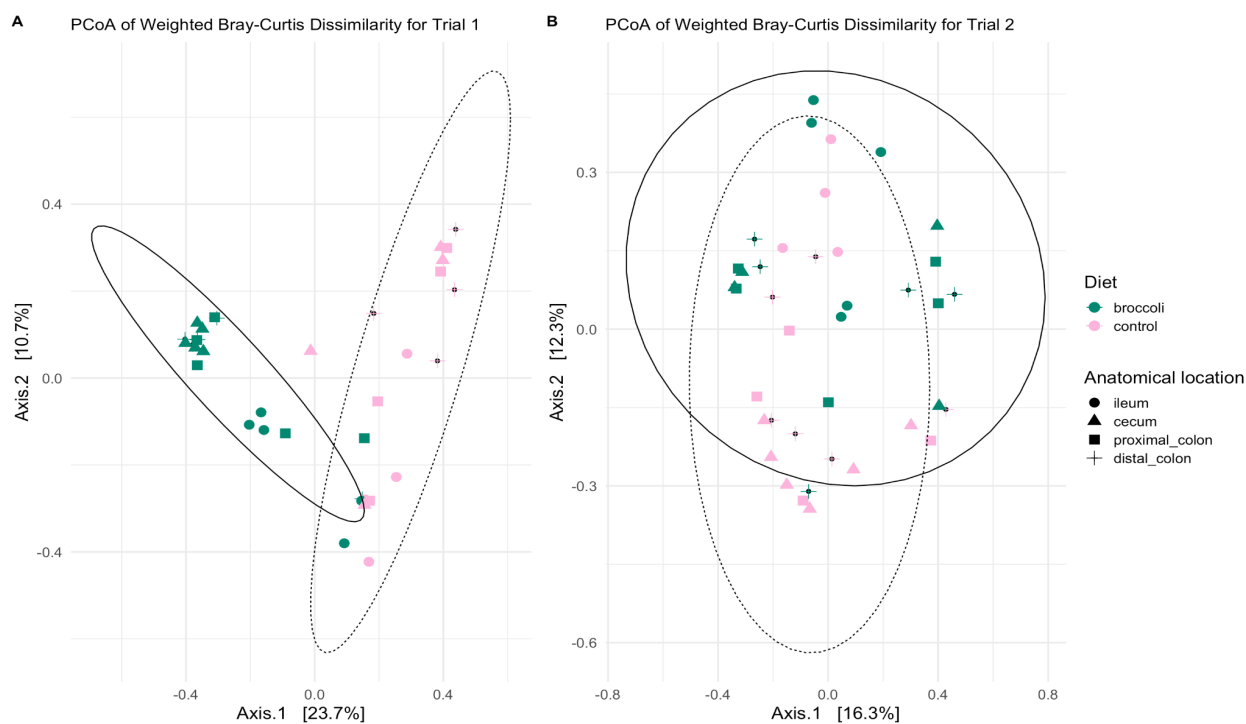


**Figure 5. Principal coordinates analysis of bacterial community similarity within the gastrointestinal tracts of 4- or 7-week-old IL-10-ko mice fed control diets or broccoli sprout diets.** Calculations using weighted Bray-Curtis dissimilarity show differences in the taxonomic structure of trial 1 mice in Panel A, and trial 2 mice in Panel B. Graphic made using phyloseq, and vegan packages in R.

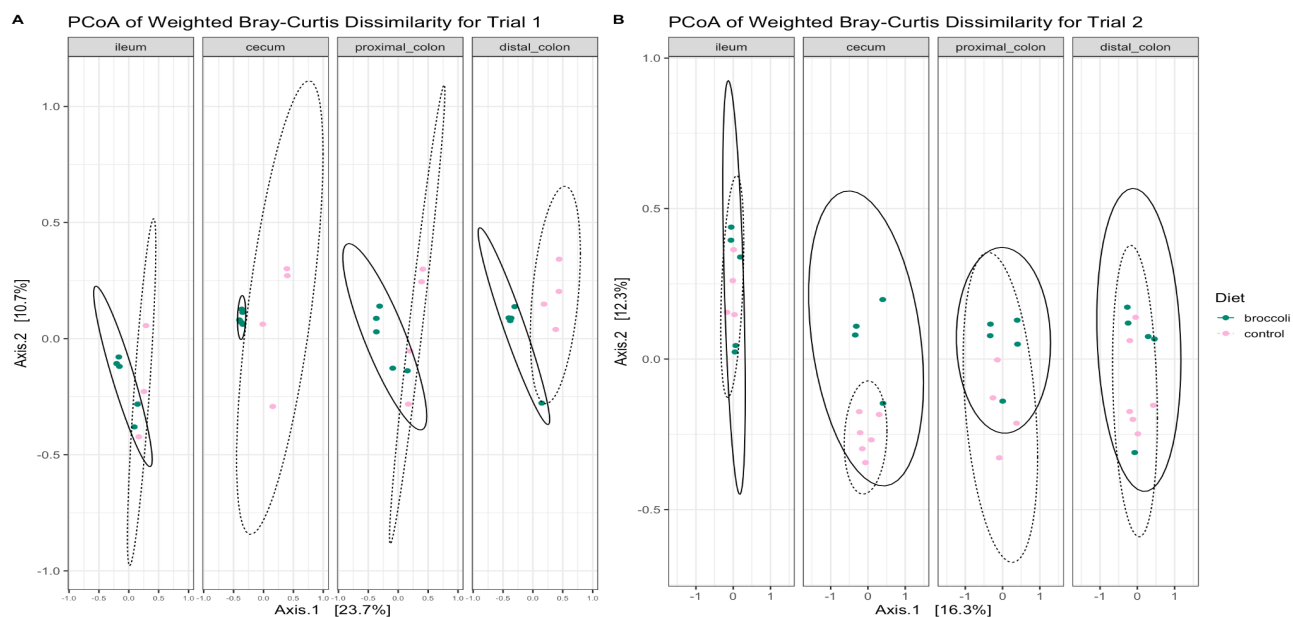


**Figure 6. Bacterial community dissimilarity within a specific anatomical location along the gastrointestinal tract of IL-10-KO mice fed control diets or broccoli sprout diets beginning at 4 or 7 weeks of age.** Calculations using weighted Bray-Curtis dissimilarity show differences in the taxonomic structure of (A) trial 1 mice sampled at age 6 weeks, and (B) trial 2 mice sampled at age 9 weeks, after each had been consuming diets for 3 weeks. Principal coordinates analysis graphic made using phyloseq, and vegan packages in R.

**Table 1. Statistical comparison of principal coordinates analysis of bacterial community similarity within the gastrointestinal tracts of 4- or 7-week-old IL-10-KO mice fed control diets or broccoli sprout diets.** Comparisons were done using dietary treatment and anatomical locations as factors, and subsetting by trial, as well as by anatomical location, as noted. Unweighted Jaccard Similarity and weighted Bray-Curtis metrics were used to calculate beta diversity. Number of permutations = 9999.

<u>PerMANOVA Tests of Dissimilarity</u>	Df	Test type	Trial 1, aged 4-6 weeks		Trial 2, aged 7-9 weeks	
			F	P-value	F	P-value
<b>Diet</b>	1	Jac	2.7779	0.0001***	1.1898	0.0258*
		BC	7.5867	0.0001***	2.4498	0.0022**
<b>Anatomical Location</b>	3	Jac	1.2027	0.0291*	1.0955	0.0359*
		BC	1.5991	0.0205*	1.4958	0.0139*
<b>Diet: Anatomical Location</b>	3	Jac	1.0704	0.1780	0.9559	0.8477

		BC	1.0482	0.3504	0.8272	0.8300
<b>Diet effect within ileum</b>	1	Jac	1.1319	0.1242	1.0154	0.3133
		BC	1.4445	0.1220	1.3366	0.1699
<b>Diet effect within cecum</b>	1	Jac	1.9352	0.0074**	1.0393	0.2663
		BC	4.4036	0.0081**	1.6667	0.0818
<b>Diet effect within proximal colon</b>	1	Jac	1.3499	0.0554	0.9949	0.3998
		BC	2.0148	0.0247*	0.8776	0.6080
<b>Diet effect within distal colon</b>	1	Jac	1.7018	0.0261*	1.0058	0.4183
		BC	4.1923	0.0158*	0.9797	0.4679

Significance codes:  $p \leq 0.001$  \*\*\* |  $p \leq 0.01$  \*\* |  $p \leq 0.05$  \*

Jaccard dissimilarity = “Jac” | Bray-Curtis dissimilarity = “BC”

#### Raw broccoli sprout diet was bacteriostatic against putative pathogens

The raw broccoli sprouts had been ground and processed to prepare the diet, a process which had released broccoli myrosinase in plant tissues and metabolized the GLR to SFN prior to feeding the diet. Sulforaphane is bacteriostatic against common gut pathogens, including *Esherichia coli*, *Klebsiella pneumonia*, *Staphylococcus aureus*, *S. epidermidis*, *Enterococcus faecalis*, *Bacillus cereus*, and *Helicobacter* spp., which can be commensal in immune-competent mice (41, 42). Using that previous literature, we identified these pathogens in our mouse gut samples (Figure 7). The control groups contained more putative pathogenic genera, across more locations in the gut, and in higher abundance than the broccoli sprout groups. The younger broccoli-sprout fed mice contained less abundance of these genera than older mice.

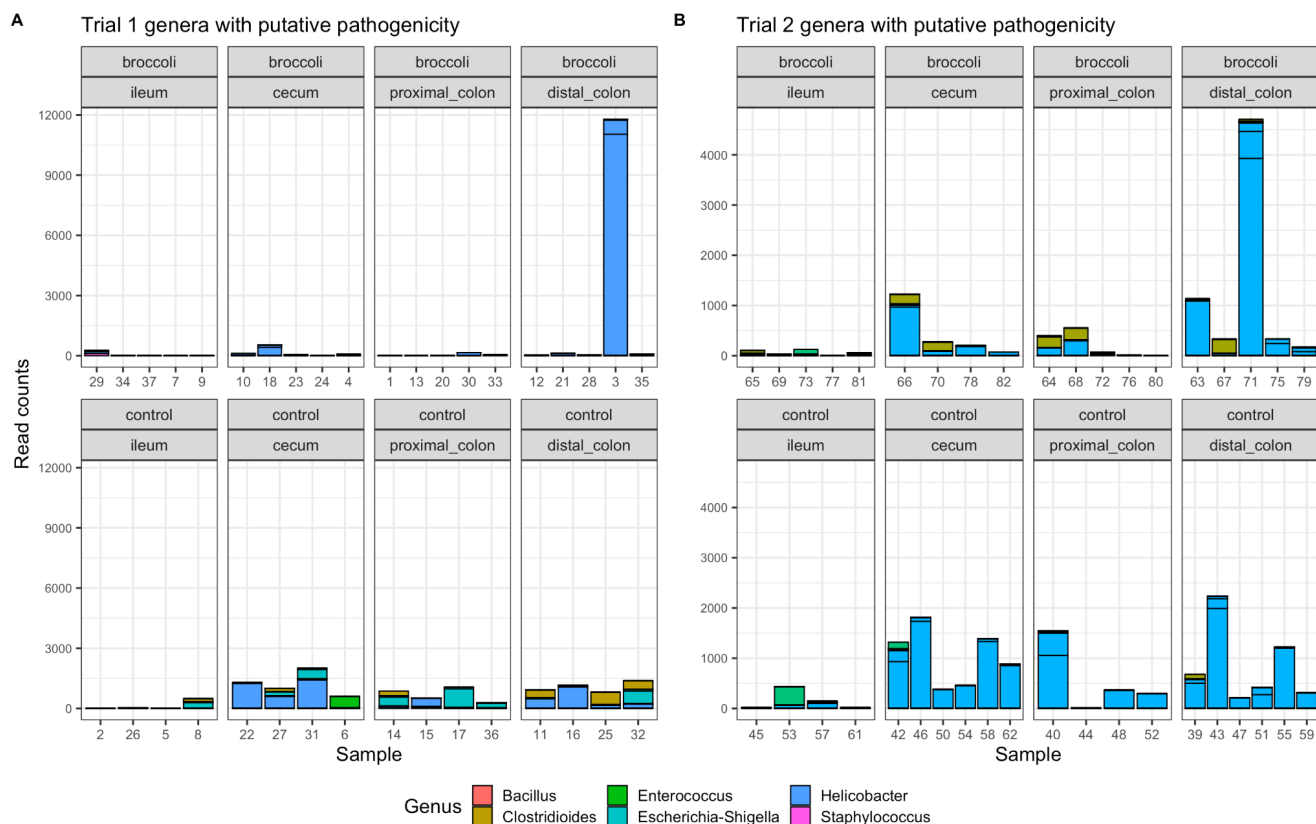


**Figure 7. Bacterial sequence variants (SVs) of genera which have putative pathogenicity.** Trial 1: 36 samples and 107 SVs; Trial 2: 39 samples and 103 SVs. Graphic made using phyloseq and ggplot2 packages in R.

### *Bacteroides* and *Lactobacillus* are present in disease models

Several bacterial taxa have the capability to perform myrosinase-like enzymatic activity and metabolize glucoraphanin into sulforaphane. After consulting the current available literature, we identified 19 taxa to analyze in detail (38, 85, 86). From our samples, we identified 562 SVs belonging to the following genera: *Bacillus*, *Bacteroides*, *Enterococcus*, *Lactobacillus*, *Lactococcus*, *Pseudomonas*, and *Staphylococcus* (Figure 8). Though, we did not find *Bifidobacterium*, *Listeria*, *Pediococcus*, *Streptomyces*, *Aerobacter*, *Citrobacter*, *Enterobacter*, *Escherichia*, *Salmonella*, *Paracolobactrum*, *Proteus*, or *Faecalibacterium*. There were few putative GSL-converting taxa found in the younger trial 1 mice fed the broccoli sprout diet, however, there were high numbers of read counts for *Bacteroides* and *Lactobacillus* in the trial 1

controls. Both dietary treatment groups of the older trial 2 mice exhibited high levels of *Bacillus* and *Enterococcus* SVs (Figure 8).

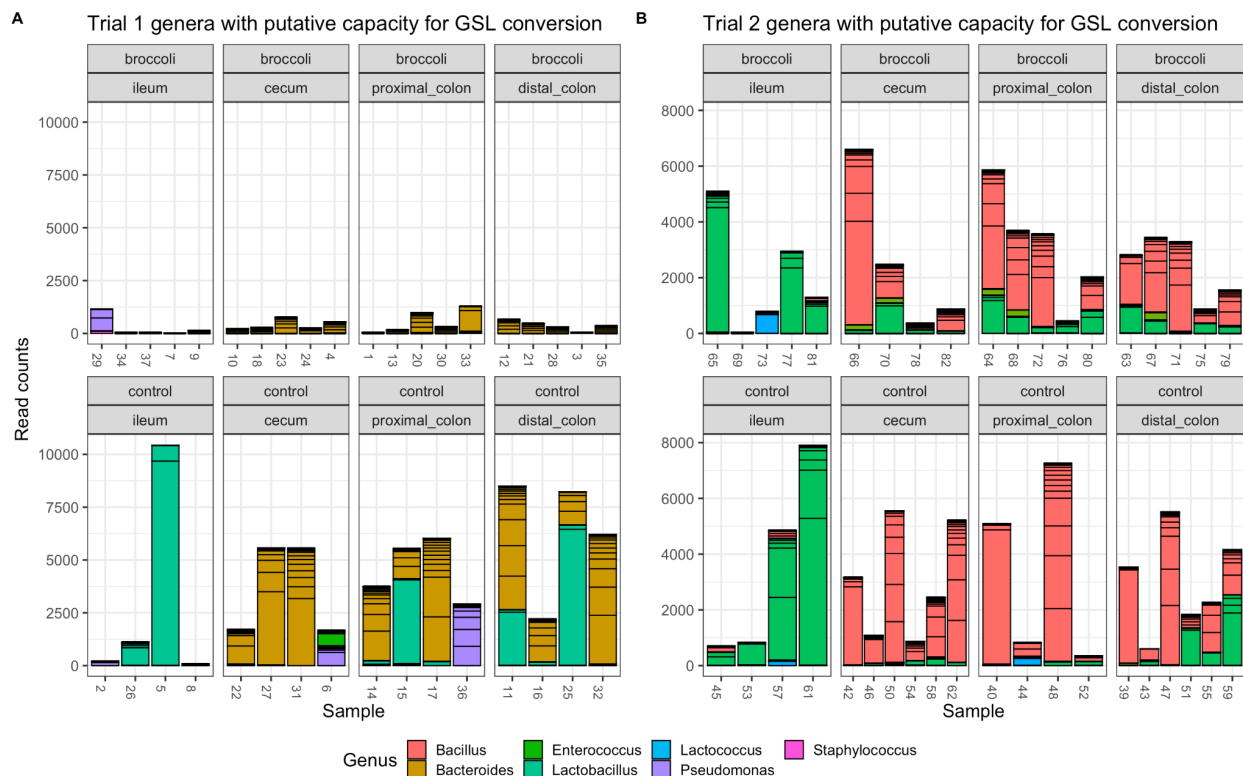


**Figure 8. Bacterial sequence variants (SVs) of genera which have putative capacity to convert glucoraphanin to sulforaphane (GSL).** Strains of bacteria in these genera have been demonstrated to perform myrosinase-like activity in the digestive tract, as reviewed in (43). Trial 1: 36 samples and 241 SVs; Trial 2: 39 samples and 353 SVs. Graphic made using phyloseq and ggpplot2 packages in R.

There were few species from putative GSL-converting genera found in the younger trial 1 mice fed the raw broccoli sprout diet (Fig. 9). The cecum and distal colon had a significant presence of *B. sartorii* and *B. acidifaciens*. The proximal colon included *B. caecimuris*, *B. sartorii*, and *B. acidifaciens*. The ileum species were mostly not identified. By contrast, the trial 1 control group had significant presence in four of the identified GSL-converting species (*Lactobacillus gasseri* in the ileum, proximal and distal colon; *B. sartorii*, *B. caecimuris*, and *B. acidifaciens* in the cecum, proximal and distal colon).

In the older trial 2 mice, the overall presence of GSL-converting taxa was similar to the trial 1 control, but with five of the identified species having significant presence (Fig. 9). In the trial 2 broccoli fed mice, the highest presence was *Lactobacillus intestinalis* in the ileum with less but still significant presence in the cecum, proximal and distal colon. These mice also had a significant presence of *B. caecimuris* and *B. acidifaciens* in the cecum, and proximal and distal colon, with *B. sartorii* in the proximal and distal colon. As in the trial 1 control, the trial 2 control had a high presence of *L. gasseri* in the ileum, but there was much less in the proximal and distal colon. *B. acidifaciens* was dominant in the cecum, proximal and distal colon. *L. intestinalis* had a significant presence in the ileum, cecum, and distal colon as did *B. sartorii* in cecum, proximal and distal colon. There was a minor presence of *E. casseliflavus*, *E. faecalis*, *B. thetaiotaomicron*, *E. cecorum*, and *S. aureus*.

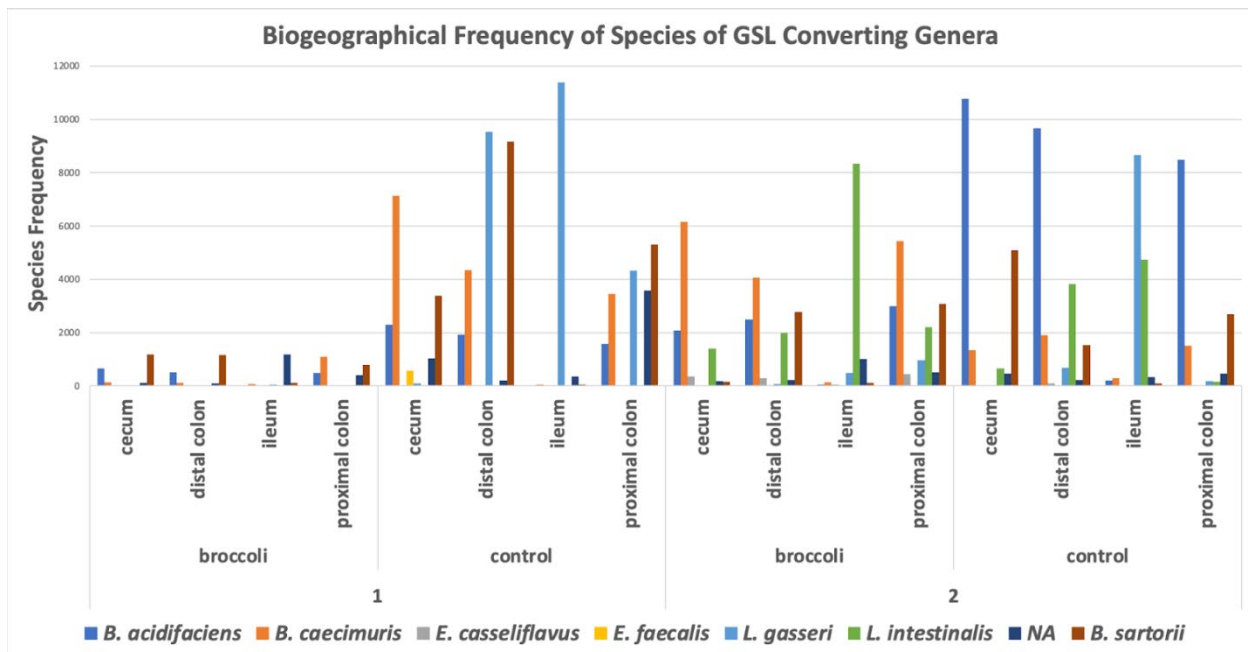


**Figure 9. Biogeographic frequency of species from putative GSL-converting genera in the treatment groups.** The Silva Database identified *Bacteroides* species *acidifaciens*, *caecimuris*, and *sartorii*, *Enterococcus cecorum*, *Staphylococcus aureus*, and *Lactobacillus intestinalis*. NCBI BLASTN identified additional *B. acidifaciens*, *B. caecimuris*, and *B. sartorii*. BLASTN uniquely identified *Enterococcus* species *casseliflavus* and *faecalis*, and *Lactobacillus gasseri*. *Bacteroides thetaiotaomicron* was linked to two (2) SVs based on genome mapping. *E. cecorum*

(frequency 12), *S. aureus* (2), and *B. thetaiotaomicron* (5) were not included in the figure as their frequencies were minimal.

## Discussion

The objective of this pilot study was to evaluate IL-10 deficient mice as a model for studying the role of dietary broccoli and broccoli bioactives in reducing inflammation, modifying the immune response, and supporting gastrointestinal tract microbial systems. Diet is well-recognized to drive gut microbial diversity, and in particular, high-fiber diets can increase microbial diversity, recover beneficial symbiotic species in the gut, and reduce inflammation by providing antioxidants against reactive oxygen species or antimicrobials against microbial competitors. Our initial hypothesis was that a medium-high concentration of raw broccoli sprouts in the diet of mice would induce changes to the gut microbiota, increase SFN present in the plasma, and collectively reduce the symptoms of enterocolitis. In conducting two replications of a diet trial, we observed a previously unreported effect of age in early life – a three week difference – on the response to broccoli sprout bioactives.

Dextran sodium sulfate (DSS) is an established and widely used model for studying SFN reduction and prevention of IBD in animals (22, 23). Treatment of DSS in drinking water results in a disease profile similar in progression and morphology to human Ulcerative Colitis (22, 44). DSS colitis begins by modifying the expression of tight junction proteins in intestinal epithelial cells, leading to a leaky epithelial barrier (45). This is followed by goblet cell depletion, erosion, ulceration, and infiltration of neutrophils into the lamina propria and submucosa (46), triggering the innate immune response (47, 48). However, Bhattacharyya et al reported DSS treatment results in an excess of ROS species which quickly dephosphorylate Hsp27 resulting in direct I $\kappa$ B $\alpha$  dissociation, circumventing the canonical inflammatory pathway (49). Further, DSS treatment instigates colitis through chemical and physical damage, without a direct interaction on the

immune system, thus it is inadequate for investigating the specific immunohistopathology present in Crohn's Disease. While a few studies have used IL-10-ko mice to study the effects of certain mineral additives (50, 51), isomaltodextrin supplementation (52), or high-fat diets on colitis (53, 54), the use of this model for diet studies is still nascent.

#### Younger IL-10-KO mice were more responsive to diet compared to adolescent counterparts

A key finding from the bacterial community analyses performed in this study was that bacterial richness and community similarity were greater in younger mice (4 - 6 weeks old during trial 1) than in adolescent mice (7 - 9 weeks old during trial 2) after three weeks on either the broccoli or control diet, and that the difference between raw broccoli sprouts and control diets was significant in the younger mice but not in older ones. We hypothesized that the responsiveness of young mice to our dietary treatment was driven by the instability of the developing gut microbiota and its amenability to selective pressures. Mice wean at approximately 20-22 days of life (3 weeks) and this time period is critical for the development of the neonate's immune system and gut microbiota, a community succession which is coordinated by immune factors in milk, growth of the gastrointestinal tract, and improvement of epithelial barrier function (55). By 28 - 35 days of life (4 - 5 weeks), mice are just beginning sexual development but are still juveniles, and still have a changing gut microbiome (56). By days 35 - 42 (5 - 6 weeks) they are beginning adolescence (57), and during this period their gut microbiome stabilizes and will remain through adulthood unless it is perturbed (56). Thus, our trial 1 mice were still in a transitional state of life and trial 2 mice were just beginning a period of life marked by stability of the immune system and gut microbiome. Our findings are consistent with previous human studies that have suggested that gut microbiota of infants and children are more plastic than that of adults (11). In humans, starting around age 3, gut microbiota fall into long-term patterns driven by consistency in diet and lifestyle (11, 58-60).

In mouse models, events in early life like stress, e.g., (61), antibiotics, e.g., (62), or other disruptions like colitis, e.g., (63), are shown to negatively impact microbial communities well into adulthood. IL-10-ko mice will acquire a microbiota as they age if they are placed in non-sterile rearing conditions (64), but even when they acquire microbiota they appear to never fully develop diverse, commensal gut microbiota and this appears to be attributable to the spontaneous generation of enterocolitis at the 4 - 6 weeks of age (65). In humans, IBD is partly linked to certain disruptions in early life, including exposure to antibiotics (5) or cigarette smoke (4), and being fed formula instead of breastmilk (4).

In their review article, Derrien et al. highlight the importance of diet in microbiota development in early life (11). Consumption of foods rich in fiber, such as fruits, vegetables, and grains, has been associated with microbiota stabilization (60), because the wealth of microbial byproducts is demonstrated to recruit and maintain a diverse microbial community (66), reduce inflammation, improve nutrition, and stimulate gut motility: aspects which are limited in IBD (67–69). Furthermore, in adults, undergoing dietary change is one of the few external factors that can “destabilize,” or subject the adult gut microbiota to change (11, 59), which may be useful in removing gut microbial communities which are not providing functional benefits and recruiting a different community instead.

#### Raw broccoli sprouts increase microbiota richness and diversity while possibly reducing proinflammatory bacteria

A functional gastrointestinal tract has a stable community of gut symbionts, composed mainly of bacteria, which provides support for digestion, immune function, and which can resist infiltration and infection by pathogenic microorganisms and protect against metabolic disease (70). Inflammatory diseases such as CD are associated with changes in the presence, abundance, and functionality of a patient's microbiomes (68, 71, 72). Studies in CD have shown

population clustering and reduced bacterial taxonomic diversity within the Firmicutes and Bacteroidetes phyla (73), both of which are dominant in the gut and are indicators of broad-changes to the gut community. Additionally, CD has specifically been associated with a reduction in *Faecalibacterium prausnitzii*, a putative glucosinolate metabolizer, and reintroduction of this bacteria resulted in decreased inflammation (74). However, not all studies on the gut microbiota in IBD patients point to specific patterns of change across all disease states and people, and many gut microbiota are only useful to the host in specific metabolic conditions (75, 76), which can obfuscate our understanding of which microbiota may be useful to try and maintain in order to preserve beneficial interactions with the host.

After subsetting our data by trial (age), we found that dietary treatment was the next most significant driver of bacterial community structure (Table 1). We observed that mice fed broccoli sprouts had greater bacterial community richness when compared to the control group. Also, compared to the controls, the younger mice fed a diet containing broccoli sprouts had more bacterial genera meet the core genera standard of prevalence and abundance (Figure S5). This finding is of interest because it may suggest that young age and/or a broccoli diet promote a larger, more diverse core community of bacteria within the diseased gut of our mouse models. We also found that the broccoli-fed mice of trial 2 had fewer genera that met the core standard, which could suggest that the core gut microbial community diminishes with age.

Interestingly, our results suggest that consumption of broccoli sprouts may prevent the accumulation of putatively harmful, pro-inflammatory bacteria. When compared to the controls, the broccoli-fed mice exhibited less prevalence and abundance of *Helicobacter*, which maybe act is a non-harmful commensal in conventionally raised and immune competent mice, but acts as a pro-inflammatory bacterial genus in IL-10-ko mice with little ability to moderate their own response to the presence of microbiota (35). The specific species of *Helicobacter* which colonies IL-10-ko mice can also affect the host's immune response and severity of symptoms (77). Sulforaphane is bacteriostatic against several bacteria, including *Escherichia coli*, *Klebsiella pneumonia*,

*Staphylococcus aureus*, *S. epidermidis*, *Enterococcus faecalis*, *Bacillus cereus*, and *Helicobacter* spp. (41, 42, 78).

Sulforaphane is also bacteriostatic against bacterial taxa which may provide some benefit to mice, including *Bacteroides* (79), a genera containing known glucosinolate metabolizers (80). Across many of our experimental groups, we found several bacterial genera, including *Bacteroides* (but not *Bacteroides thetaiotaomicron*), *Enterococcus casseliflavus*, *Lactobacillus gasseri*, and others in very low abundance, that may perform myrosinase-like activity in the digestive tract (Figure 8), as reviewed in (43). *Enterococcus casseliflavus* are gram-positive, motile facultative anaerobes sourced from vegetables, with high glucosinolate degradation efficiency (81). One (1) SV was matched to *E. casseliflavus* based on BLASTN results in the trial 2 mice, and favored the broccoli mice in trial 2 (1164 count) compared to the control (113). Although GLR levels were low in the broccoli group (4  $\mu$ g on average), *E. casseliflavus* may have been responsible for some of the conversion to SFN.

*Lactobacillus gasseri* was the most abundant species with putative myrosinase-like enzymatic activity. A probiotic strain with implications for fighting pathogens, *L. gasseri* has hydrolyzed GLR to SFN *in situ* in the cecum of rats (82, 83). Four (4) SVs were mapped to *L. gasseri* using BLASTN. These sequences were most abundant in the control for both trials (trial 1: 25342 vs. 97; trial 2: 9567 vs. 1532), with the highest counts occurring in the younger trial 1 control mice.

Contrary to expectations, with the exception of *Bacteroides caecimuris*, *Enterococcus casseliflavus*, and *Lactobacillus intestinalis*, the species identified from GSL converting genera tended to favor the control treatments for both trial 1 and 2. As a whole, the presence of GSL genera negatively correlated with the broccoli treatments. The high concentration of SFN in the diet, and the relatively low amount of the GLR precursor, may have precluded the need to select for metabolizing-competent bacteria, and it may be that the taxa present in younger mice were sensitive to the presence of SFN while the community present in older mice was not. However, in

these mice without the ability to recruit commensal bacteria, commensalism cannot be assumed for any taxa. For example, IL-10-ko mice infected with *Helicobacter* also exhibited higher abundance of *Bacteroides* and *Lactobacillus* species (84).

#### Biogeographical patterns emergent in younger mice consuming broccoli sprouts

Anatomical location within the gut, including different organs and solid-associated, liquid-associated, and mucosal-associated locations, select for different bacterial communities due to environmental conditions and anatomical features specific to each location, i.e. biogeography (85–87), even within the first few days of life, e.g. (88). In IL-10-ko mice, which are raised in ‘germ-free’ conditions and do not acquire gut microbiota, there is no biogeographical signal in the gut, and the damage to the epithelium caused by inflammation or the lack of IL-10 may preclude the ability of a typical biogeographical signal to form. The addition of a conventionally raised mouse to the IL-10-ko mouse cages, and placement in a conventional mouse room, is enough to stimulate microbial transmission (89) and for IL-10-ko mice to acquire a gut microbiota even as they react negatively to it.

The third experimental factor of this study, and the one that showed to be the least significant driver of microbial community dissimilarity, was the anatomical location of sample derivation. We found that the number of bacterial taxa (SVs) in the cecum and proximal colon of the younger trial 1 mice fed broccoli sprouts was significantly elevated, as compared to the control trial 1 mice (Figure 4B), and significant community dissimilarity between the broccoli sprout diet group the control group in both the cecum and the distal colon. There were no significant dietary treatment effects on richness or bacterial community similarity in any anatomical location studied in the older trial 2 mice (Figure 4B). The cecum, a muscular and oblong pouch emerging from the junction of the ileum and proximal colon, houses a diverse community of fibrolytic bacteria, and specialized peristaltic movements allow for fiber in the ileocecal junction to be pulled into the cecum, as well as separate large and small fibers to allow for retention of particles to induce more

microbial fermentation. Mice have a large cecum, even in IL-10-ko mice this organ acquires a diverse microbiota given enough microbial exposure and time (64). Studies on inflammation for IBD models report significant inflammation and changes to cecal microbiota in mice (21, 90, 91). It is likely that given the short duration of this experimental period, the cecum and parts of the colon that also house diverse microbiota were the only organs which were suited to recruit differential bacterial communities fast enough to be statistically significant. While humans have a very small cecum relative to our size, and do suffer inflammation there in IBD patients, the effect on IBD of the microbiota there is unknown.

### Limitations and Future Directions

In our study, raw broccoli sprouts in the diet provided during the critical period of microbiome stabilization and enterocolitis development in these IL-10-ko mice resulted in an increase in microbial diversity. Due to the short duration of the experiment, we were unable to discern if this increase in diversity persists into adulthood, and if this would preclude the development of more intense symptoms and damage to the intestinal epithelium. Further, we lacked sufficient power to determine sex specific differences in response to diet (52, 92), immune function (93), and microbial acquisition (94).

Future research will also be required to examine the effect of cooking preparation on the concentrations of precursors and bioactives which are contained in the diet and available in the gut. The myrosinase enzyme present in broccoli and sprouts can metabolize the glucoraphanin precursor to bioactive SFN when the plant tissues are cut or chewed, but most of the precursor is converted to biologically inactive SFN nitrile by the epithiospecifier protein, also present in broccoli (9). SFN was high in our raw sprout diet, which was an effect of the preparation process stimulating release of myrosinase. However, SFN is an unstable molecule and will not persist in processed raw sprouts unless kept frozen. These enzymes can be inactivated by cooking,

preserving the stable precursor in the diet and allowing gut microbiota to perform the conversation in the intestines (20).

Future research will also be needed into the feasibility and adoptability of this intervention. The difficulty in managing CD symptoms is costly: patients spend an average of \$2,000 USD/year on out-of-pocket costs (95), and collectively create billions in U.S. healthcare costs (96, 97). Further, many IBD patients may be told to avoid fiber for fear of exacerbating symptoms or aggravating tender intestines (18, 24). Given the importance of diet in supporting host health and microbiota, we underscore the need for understanding dietary preferences, and for incorporating nutritional intervention as part of a holistic treatment for gastrointestinal inflammation.

## **Materials and Methods**

### Diet

Multiple lots of Jonathan's Sprouts™ (Rochester, MA, U.S.) broccoli sprouts were purchased from a nearby grocery store (Bangor, ME, U.S.) and stored in a -70°C freezer for storage until they could be freeze-dried at the University of Maine Pilot Plant (Orono, ME, U.S.). The sprouts were then crushed by mortar and pestle into a fine powder and mixed with purified 5LOD rodent diet powder and water to a concentration of 10% by weight. Our labs have assessed the effects of different diet preparations and the percentage of broccoli sprouts, and found that 5-10% broccoli sprouts by weight reliably produces consistent anti-inflammatory results (98). Diet pellets were formed using a silicone mold to ensure consistent sizing, and allowed to dry at room temperature for up to 48 hours in a chemical safety hood to facilitate moisture evaporation, and after drying were stored in ziploc bags in a -10°C freezer until future use. Samples from the control and the sprout diet were tested for glucoraphanin and sulforaphane concentrations using LC/MS (20), none was found in the control and the sprout diet contained an average 4 µg of GLR and 85

µg of SFN (induced when raw diets are crushed and myrosinase is released from broccoli tissue vesicles).

### IL-10 Mouse Model

All experimental protocols were approved by the Institutional Animal Care and Use Committee of the University of Vermont (PROTO202000040), in Burlington, Vermont, U.S. and all biosafety work at the University of Maine was approved by the Institutional Biosafety Committee (protocol SI-092220). Two replicate trials were conducted using male and female IL-10 knockout mice (*Mus musculus*) on a C57BL/6 background (B6.129P2-Il10tm1Cgn/J, strain 2251; Jackson Laboratories, Bar Harbor, Maine, U.S.). IL-10-ko mice are a well-demonstrated model for Crohn's research and the C57BL/6 genetic line shows some genetic-based resistance to developing symptoms (32), which allowed us to focus on environmental triggers of disease.

Trial 1 included 9 mice starting at 4 weeks of age, which is younger than usual, due to the age of available mice at the time when a trial could be conducted. Trial 2 included 10 mice starting at 7 weeks of age, which is the standard age for IL-10 microbiota trials.

The experimental design was structured as a prevention paradigm (Figure 1). A colony of homozygous interleukin-10 knockout mice was maintained in a barrier facility which is *Helicobacter (H.) hepaticus* free. Beginning at the start and for the duration of the trial, they were given *ad libitum* either the 5LOD control diet or the treatment diet consisting of 10% by volume raw broccoli sprouts and 90% control diet. Mice had access to autoclaved tap water *ad libitum*. Mice consumed the respective diets for 7 days to allow them to acclimate, prior to the induction of colitis, and remained on their respective diets for the remaining 16 days of the experiment while they developed symptoms.

After the 7 day diet acclimation period, IL-10-ko mice were moved to a conventional mouse room for a period of one week, after which a *H. species*-positive mouse was added to the IL-10 mouse cages for one day, to transfer commensal bacteria and induce colitis over the course of

10 days (32, 39). In the first trial, at 4 weeks of age which is just after the weaning period, experimental IL-10-KO mice were moved to a conventional mouse room. In the second trial, IL-10 mice were older than anticipated when the trial began, and were moved to a conventional mouse room at 7 weeks of age. Day 0 of each trial was set as the day the IL-10 mice were exposed to the conventional mouse, such that experimental Day 10 is when symptoms appear (Figure 1). Animals were euthanized by carbon dioxide and cervical dislocation on Day 16.

### Assessment of Disease Activity

Disease severity was assessed every other day beginning on Day 0 when mice were conventionalized, using a disease activity index (DAI), which includes an evaluation of weight loss/stagnation, fecal blood presence and severity, and stool consistency (99). The animals' weights were normalized to their baseline weight on Day 0 of the trial, as at this age, mice are still in a growth phase and likely to gain weight even when under duress. The presence of fecal blood was assessed using Hemocult Single Slide testing slides (Beckman Coulter, Brea, CA, U.S.).

Fecal samples were also collected and frozen at various time points for evaluation of fecal lipocalin (LCN2); a neutrophil protein that binds bacterial siderophores and serves as a biomarker for intestinal inflammation (40). Frozen fecal samples were weighed to 20 mg and reconstituted in phosphate buffered solution (PBS) with 0.2 mL of 0.1% Tween 20. Samples were then thawed and vortexed to create a homogenous fecal suspension. The samples were centrifuged for 10 minutes at 12,000 rpm at 4 °C. Clear supernatant was collected and stored at -20 °C until analysis. Lipocalin-2 concentration, a neutrophil protein that binds bacterial siderophores and serves as a biomarker for intestinal inflammation (40), was measured in the samples by a mouse Lipocalin-2/NGAL DuoSet ELISA kit (R & D Biosystems, USA) following the manufacturer's instructions. The readings at wavelengths of 540 nm and 450 nm were measured by a Thermo Scientific Varioskan LUX Multimode Microplate Reader. Serum was collected from mice after euthanasia, and measured for sulforaphane concentration using LC/MS (20).

## Histological Analysis of Tissues

After euthanasia, tissue segments (1 cm, collected in duplicate) from the ileum, proximal colon and distal colon were collected and fixed in 4% paraformaldehyde overnight for histological evaluation. Tissues were immediately rinsed with phosphate buffer solution (PBS), placed in 2% paraformaldehyde/0.2% picric acid as a preservative, and stored at 4°C until transport to the University of Maine Electron Microscopy Laboratory (Orono, Maine) for processing. All processing protocols took place in a biosafety cabinet using aseptic techniques to reduce contamination. A pipette was used to gently remove the previous PBS that the tissue was submerged in without disturbing tissue while leaving a little bit of PBS behind to prevent the tissue drying out. The sample tubes were refilled with fresh PBS, and the wash step was repeated four times throughout the day every three hours with samples stored at 4°C between washes.

After the final wash step, the tissue samples were moved from 4°C to room temperature (25°C) and transferred from their tubes into embedding baskets. The samples were introduced to gradually increasing concentrations of ethanol (EtOH) to rinse off the PBS: first the samples were placed in a 1000 ml beaker containing a 50% EtOH solution and stored at 4°C for 2 hours, after which the solution was removed and replaced with 70% EtOH for 2 hours. This process was repeated for 80% EtOH and 96% ethanol solutions. The samples remained immersed in 96% EtOH overnight at 4°C. Multiple washes of fresh 100% EtOH were performed at 25°C (20 min, 20 min, and 60 min) to ensure no PBS remained. The samples were placed in 100% acetone for 17 min to serve as a transition solution, and then placed in two rounds of xylene for an hour each.

The prepared tissue samples in their embedding baskets went through a series of Paraplast X-tra paraffin wax warmers to rinse off the xylene before molding into wax molds were pre-folded out of paper. The tools (porous, metal ladles) were kept warm under an incandescent lightbulb to prevent wax cooling so paraffin was not mixed between each warmer tray. The

samples spent one hour in each of four successional wax warmer trays. The tissues were then taken from their embedding baskets and oriented upright in the paper molds to which wax from the last warmer tray had been added. Once the wax developed a skin, the mold was placed in a cool water bath and allowed to solidify overnight into a block. Each wax block, containing the dissected specimen, was placed in the cassette holder of the Rotary Spencer Microtome, perpendicular to the blade. The wax was sliced until a clean cross-section ribbon was successfully removed. A paint brush was used to transfer the ribbon to a cool water bath until the desired amount was obtained. A microscope slide was used to scoop out the cross-sections from the bath. The slide was allowed to dry once organized to the desired display.

The slides were heated on the slide warmer for 15 min to melt the sample onto the slide, then stained through a time-specified solvent series in Coplin staining jars and transferred using tweezers. The slide was inserted into Xylene #1 for two minutes to melt the wax; this was repeated for Xylene #2 and Xylene #3. The slide was inserted into EtOH 100% #1 for 2 minutes; this was repeated for Ethanol 100% 2 and Ethanol 100% 3. The slide was then placed in EtOH 95% for 2 minutes and EtOH 70% for another 2 minutes. After the first EtOH series, the slide was washed with running tap water (ensuring not to rinse off the sample). The slide was then transferred to a Hematoxylin stain for 30 minutes and an acid rinse for 8 minutes. The slide was then dipped once into the bluing dip, containing 1% ammonium in H<sub>2</sub>O. The slide was transferred into Eosin y for 2 minutes to provide the background stain. The sample spent 2 minutes each in EtOH 95% #1 and EtOH 95% #2. The slide finished two more 2-minute cycles in Ethanol 100% 1 and Ethanol 100% 2. The slide sat in Xylene #1 for 2 minutes; this was repeated for Xylene #2 and Xylene #3. Once removed and dried, the sample was mounted to the slide with a coverslip. One drop of SIGMA DPX Mountant for Histology was placed on each cross-section using a wooden applicator. Coverslips were placed over the cross-sections.

The tissues were scored with 7 criteria (Figure S1) used to assess inflammation in the ileum, and the proximal and distal colon tissues, performed according to parameters provided by

the Mawe Lab at the University of Vermont (100). Epithelial damage and architectural changes were scored from 0 (no damage) to 2 (extensive damage). Similarly, infiltration of mononuclear cells in the lamina propria was scored on a scale of 0 (no infiltration) to 2 (extensive infiltration). Infiltration of polymorphonuclear cells in both the lamina propria and the epithelium were scored on a scale of 0-2, with 0 indicating no infiltration, 1 equating to sighting of  $\geq 1$  cell in a given viewing field, and 2 equating to  $>3$  cells in a given viewing field. Abscesses, ulcers, erosion, and branched crypts were scored together with 0 being absence of these damage indicators and 1 being presence. Finally, presence of granulomas was scored with 0 indicating no granulomas and 1 equating to  $\geq 1$  granulomas.

#### DNA extraction and 16S rRNA bacterial sequencing library preparation

On Day 16, following euthanasia, intestinal tissue segments (2 cm in length) were collected from the ileum, cecum, proximal colon, and distal colon, and placed in RNAlater preservative (Invitrogen, Waltham, MA, U.S.) and transported overnight on ice to the University of Maine for DNA extraction. All DNA extraction processing steps took place in a biosafety cabinet using aseptic techniques to reduce contamination. All tissues containing their resident gut microbiota were gently homogenized with vortexing, then treated with propidium monoazide (PMA; BioTium) following kit protocols at a final concentration of 25  $\mu\text{M}$ . PMA covalently binds to relic/free DNA and DNA inside compromised/dead cell membranes, and prevents amplification in downstream protocols to preclude dead DNA from the sequence data.

Following PMA treatment, bulk DNA was extracted from tissue-associated bacterial communities ( $n = 80$  samples), or no-template (water) control samples ( $n = 4$ , one for each extraction batch) using commercially available kits optimized for fecal-based microbial communities (Zymo fecal/soil kit), and some aliquots archived. DNA extract was roughly quantified and purity-checked with a Nanodrop spectrophotometer. Samples underwent DNA amplicon sequencing of the 16S rRNA gene V3-V4 region, using primers 341F (101) and 806R

(102) and protocols consistent with The Earth Microbiome Project (103), and sequenced on an Illumina MiSeq platform using the 2 x 300-nt V3 kit (Molecular Research Labs, Clearwater, TX). Nine samples failed the first sequencing run, and were extracted again for repeated sequencing. Raw sequence data (fastq files and metadata) from both runs are publicly available from the NCBI Sequence Read Archive (SRA) under BioProject Accession PRJNA909836.

### 16S rRNA bacterial community sequencing analysis

Amplicon sequence data was processed using previously curated workflows in the Ishaq Lab (Supplemental Material) which used the DADA2 pipeline ver. 1.22 (104) in the R software environment ver. 4.1.1 (105). The dataset started with 38,287,212 million raw reads from 80 samples and 4 negative controls. All samples were sequenced in an initial batch together, but 5 samples failed to meet all quality control standards and were resequenced. The two sequencing batches were put through quality control steps separately in DADA2 and combined before rarefaction. Trimming parameters were designated based on visual assessment of the aggregated quality scores at each base from all samples (plotQualityProfile in DADA2): the first and last 10 bases were trimmed, and sequences were discarded if they had ambiguous bases, more than two errors, or matching the PhiX version 3 positive control (Illumina; FC-110-3001). After filtering, 43,382,928 paired non-unique reads and 289 samples remained.

The DADA algorithm was used to estimate the error rates for the sequencing run, dereplicate the reads, pick sequence variants (SVs) which represent 'microbial individuals', and remove chimeric artifacts from the sequence table. Taxonomy was assigned using the Silva taxonomic training data version 138.1 (106) and reads matching chloroplasts and mitochondria taxa were removed using the dplyr package (107). No-template control samples were used to remove contaminating sequences from the samples by extraction batch (108). The sequence table, taxonomy, and metadata were combined using the phyloseq package (109) to facilitate statistical analysis and visualization, representing 80 samples and 22,805 taxa. Due to the large

variability in sequences per sample which passed quality assurance parameters (range 2490 - 157,040 sequences/sample), and the knowledge that some sample types would contain much lower microbial diversity than others, the data were rarefied (110, 111) to 12,060 sequences/sample.

Normality was checked using a Shapiro-Wilkes test on alpha diversity metrics generated from rarefied data; observed richness ( $W = 0.86662$ ,  $p\text{-value} = 1.186e-06$ ) and evenness ( $W = 0.89141$ ,  $p\text{-value} = 9.775e-06$ ) were not normally distributed. Shannon diversity was also not normally distributed ( $W = 0.95012$ ,  $p\text{-value} = 0.005061$ ). Linear models were run for comparisons of alpha diversity metrics using linear models to compare by sample type, (lme4 package (112)), in which anatomical location, diet treatment, and trial (either 1 or 2) were used as factors.

Jaccard unweighted similarity was used to calculate sample similarity based on community membership (species presence/absence) and non-parametric multidimensional scaling (Trial 1 run 20 stress = 0.1940131; Trial 2 run 20 stress = 0.1748438) and tested with permutational analysis of variance (perMANOVA) by using the vegan package (113). Random forest feature prediction with permutation was used to identify differentially abundant SVs based on factorial conditions (114). Plots were made using the ggplot2 (115), ggpubr (116), and phyloseq packages.

Source Tracker algorithms which had been modified for the R platform (117, 118) were used to identify source:sink effects based on anatomical location. This was used to determine if the cecum could be the source for population sinks in the colon, as a proxy for the model's applicability to the human gut anatomical features and microbial communities. A total of 38 SVs were identified as possibly sourced from the cecum (Figure S5). Common mouse commensals, but not the putative GSL converting bacteria in the Broccoli mouse gut samples, were among those taxa identified as sourced in the cecum and sinking in the proximal or distal colon.

## Acknowledgements

All authors have read and approved the final manuscript. This project was supported by the USDA National Institute of Food and Agriculture through the Maine Agricultural & Forest Experiment Station: Hatch Project Numbers ME022102 and ME022329 (Ishaq) and ME022303 (Li); the USDA-NIFA-AFRI Foundational Program [Li and Chen; USDA/NIFA 2018-67017-27520/2018-67017-36797]; and the National Institute of Health [Li and Ishaq; NIH/NIDDK 1R15DK133826-01]. Johanna Holman was supported by ME0-22303 (Li), and Lola Holcomb was supported by US National Science Foundation One Health and the Environment (OG&E): Convergence of Social and Biological Sciences NRT program grant DGE-1922560, and the UMaine Graduate School of Biomedical Science and Engineering.

## Author Contributions

Conceptualization, S.L.I., Y.L., T.Z., G.M., P.M., G.C.; Methodology, S.L.I., Y.L., T.Z., G.M., P.M., J.H., L.H., M.H., B.L.; Software, S.L.I.; Formal Analysis, J.H., L.H., S.L.I.; M.H., A.S., T.H., B.H.; Investigation, M.H., B.L.; J.H., L.H., L.C.; A.S.; Resources, G.M., S.L.I., Y.L.; Data Curation, S.L.I., J.H., L.H.; Writing - Original Draft, J.H., L.H., S.L.I., Y.L.; Writing - Review and Editing; S.L.I., Y.L., T.Z., G.M., P.M., J.H., L.H., M.H., B.L., G.C., T.H., B.H., E.P.; Visualization, J.H., L.H., S.L.I., A.S., T.H., B.H.; Supervision, S.L.I., Y.L., T.Z.; G.M.; Project Administration, S.L.I., Y.L., G.M.; Funding Acquisition, S.L.I., Y.L., G.M. G.C.

## References

1. GBD 2016 DALYs and HALE Collaborators. 2017. Global, regional, and national disability-adjusted life-years (DALYs) for 333 diseases and injuries and healthy life expectancy (HALE) for 195 countries and territories, 1990-2016: a systematic analysis for the Global Burden of Disease Study 2016. *Lancet* 390:1260–1344.
2. Roda G, Chien Ng S, Kotze PG, Argollo M, Panaccione R, Spinelli A, Kaser A, Peyrin-

- Biroulet L, Danese S. 2020. Crohn's disease. *Nat Rev Dis Primers* 6:22.
3. Spehlmann ME, Begun AZ, Burghardt J, Lepage P, Raedler A, Schreiber S. 2008. Epidemiology of inflammatory bowel disease in a German twin cohort: results of a nationwide study. *Inflamm Bowel Dis* 14:968–976.
  4. Lindoso L, Mondal K, Venkateswaran S, Somineni HK, Ballengee C, Walters TD, Griffiths A, Noe JD, Crandall W, Snapper S, Rabizadeh S, Rosh JR, LeLeiko N, Guthery S, Mack D, Kellermayer R, Gulati AS, Pfefferkorn MD, Moulton DE, Keljo D, Cohen S, Oliva-Hemker M, Heyman MB, Otley A, Baker SS, Evans JS, Kirschner BS, Patel AS, Ziring D, Stephens MC, Baldassano R, Dubinsky MC, Markowitz J, Denson LA, Hyams J, Kugathasan S, Ananthakrishnan AN. 2018. The Effect of Early-Life Environmental Exposures on Disease Phenotype and Clinical Course of Crohn's Disease in Children. *Am J Gastroenterol* 113:1524–1529.
  5. Örtqvist AK, Lundholm C, Halfvarson J, Ludvigsson JF, Almqvist C. 2019. Fetal and early life antibiotics exposure and very early onset inflammatory bowel disease: a population-based study. *Gut* 68:218–225.
  6. Segal AW. 2019. Studies on patients establish Crohn's disease as a manifestation of impaired innate immunity. *J Intern Med* 286:373–388.
  7. Gunasekera DC, Ma J, Vacharathit V, Shah P, Ramakrishnan A, Uprety P, Shen Z, Sheh A, Brayton CF, Whary MT, Fox JG, Bream JH. 2020. The development of colitis in Il10<sup>-/-</sup> mice is dependent on IL-22. *Mucosal Immunol* 13:493–506.
  8. Jiang Y, Wu S-H, Shu X-O, Xiang Y-B, Ji B-T, Milne GL, Cai Q, Zhang X, Gao Y-T, Zheng W, Yang G. 2014. Cruciferous vegetable intake is inversely correlated with circulating levels of proinflammatory markers in women. *J Acad Nutr Diet* 114:700–8.e2.

9. Holman J, Hurd M, Moses P, Mawe G, Zhang T, Ishaq SL, Li Y. 2023. Interplay of Broccoli/Broccoli Sprout Bioactives with Gut Microbiota in Reducing Inflammation in Inflammatory Bowel Diseases. *J Nutr Biochem* 113:109238.
10. Gibbons SM, Kearney SM, Smillie CS, Alm EJ. 2017. Two dynamic regimes in the human gut microbiome. *PLoS Comput Biol* 13:e1005364.
11. Derrien M, Alvarez A-S, de Vos WM. 2019. The Gut Microbiota in the First Decade of Life. *Trends Microbiol* 27:997–1010.
12. Ostrem Loss E, Thompson J, Cheung PLK, Qian Y, Venturelli OS. 2023. Carbohydrate complexity limits microbial growth and reduces the sensitivity of human gut communities to perturbations. *Nat Ecol Evol* 7:127–142.
13. Swidsinski A, Ladhoff A, Pernthaler A, Swidsinski S, Loening-Baucke V, Ortner M, Weber J, Hoffmann U, Schreiber S, Dietel M, Lochs H. 2002. Mucosal flora in inflammatory bowel disease. *Gastroenterology* 122:44–54.
14. Duvallet C, Gibbons SM, Gurry T, Irizarry RA, Alm EJ. 2017. Meta-analysis of gut microbiome studies identifies disease-specific and shared responses. *Nat Commun* 8:1784.
15. Khan I, Bai Y, Ullah N, Liu G, Rajoka MSR, Zhang C. 2022. Differential Susceptibility of the Gut Microbiota to DSS Treatment Interferes in the Conserved Microbiome Association in Mouse Models of Colitis and Is Related to the Initial Gut Microbiota Difference. *Advanced Gut & Microbiome Research* 2022:7813278.
16. Leshem A, Segal E, Elinav E. 2020. The Gut Microbiome and Individual-Specific Responses to Diet. *mSystems* 5:e00665–20.
17. Gibbons SM, Gurry T, Lampe JW, Chakrabarti A, Dam V, Everard A, Goas A, Gross G,

- Kleerebezem M, Lane J, Maukonen J, Penna ALB, Pot B, Valdes AM, Walton G, Weiss A, Zanzer YC, Venlet NV, Miani M. 2022. Perspective: Leveraging the Gut Microbiota to Predict Personalized Responses to Dietary, Prebiotic, and Probiotic Interventions. *Adv Nutr* 13:1450–1461.
18. Lewis JD, Abreu MT. 2017. Diet as a Trigger or Therapy for Inflammatory Bowel Diseases. *Gastroenterology* 152:398–414.e6.
  19. Limdi JK. 2018. Dietary practices and inflammatory bowel disease. *Indian J Gastroenterol* 37:284–292.
  20. Zhang T, Holman J, McKinstry D, Trindade BC, Eaton KA, Mendoza-Castrejon J, Ho S, Wells E, Yuan H, Wen B, Sun D, Chen GY, Li Y. 2022. A steamed broccoli sprout diet preparation that reduces colitis via the gut microbiota. *J Nutr Biochem* 112:109215.
  21. Holman J, Holcomb L, Colucci L, Baudewyns D, Balkan J, Hunt T, Hunt B, Chen G, Moses PL, Mawe GM, Zhang T, Li Y, Ishaq SL. 2023. Steamed broccoli sprouts alleviate gut inflammation and retain gut microbiota against DSS-induced dysbiosis.
  22. Eichele DD, Kharbanda KK. 2017. Dextran sodium sulfate colitis murine model: An indispensable tool for advancing our understanding of inflammatory bowel diseases pathogenesis. *World J Gastroenterol* 23:6016–6029.
  23. Wirtz S, Popp V, Kindermann M, Gerlach K, Weigmann B, Fichtner-Feigl S, Neurath MF. 2017. Chemically induced mouse models of acute and chronic intestinal inflammation. *Nat Protoc* 12:1295–1309.
  24. Hou JK, Lee D, Lewis J. 2014. Diet and inflammatory bowel disease: review of patient-targeted recommendations. *Clin Gastroenterol Hepatol* 12:1592–1600.

25. Walker A, Schmitt-Kopplin P. 2021. The role of fecal sulfur metabolome in inflammatory bowel diseases. *Int J Med Microbiol* 311:151513.
26. Buisine MP, Desreumaux P, Debailleul V, Gambiez L, Geboes K, Ectors N, Delescaut MP, Degand P, Aubert JP, Colombel JF, Porchet N. 1999. Abnormalities in mucin gene expression in Crohn's disease. *Inflamm Bowel Dis* 5:24–32.
27. Söderholm JD, Olaison G, Peterson KH, Franzén LE, Lindmark T, Wirén M, Tagesson C, Sjö Dahl R. 2002. Augmented increase in tight junction permeability by luminal stimuli in the non-inflamed ileum of Crohn's disease. *Gut* 50:307–313.
28. Eckburg PB, Relman DA. 2007. The role of microbes in Crohn's disease. *Clin Infect Dis* 44:256–262.
29. Opiari A, Franchi L. 2015. Role of inflammasomes in intestinal inflammation and Crohn's disease. *Inflamm Bowel Dis* 21:173–181.
30. Weaver CT, Hatton RD. 2009. Interplay between the TH17 and TReg cell lineages: a (co-)evolutionary perspective. *Nat Rev Immunol* 9:883–889.
31. Nieminen U, Jussila A, Nordling S, Mustonen H, Färkkilä MA. 2014. Inflammation and disease duration have a cumulative effect on the risk of dysplasia and carcinoma in IBD: A case-control observational study based on registry data. *International Journal of Cancer* 134:189–196.
32. Keubler LM, Buettner M, Häger C, Bleich A. 2015. A Multihit Model: Colitis Lessons from the Interleukin-10-deficient Mouse. *Inflamm Bowel Dis* 21:1967–1975.
33. Duell BL, Tan CK, Carey AJ, Wu F, Cripps AW, Ulett GC. 2012. Recent insights into microbial triggers of interleukin-10 production in the host and the impact on infectious

- disease pathogenesis. *FEMS Immunol Med Microbiol* 64:295–313.
34. Glocker E-O, Kotlarz D, Klein C, Shah N, Grimbacher B. 2011. IL-10 and IL-10 receptor defects in humans. *Ann N Y Acad Sci* 1246:102–107.
  35. Burich A, Hershberg R, Waggie K, Zeng W, Brabb T, Westrich G, Viney JL, Maggio-Price L. 2001. *Helicobacter*-induced inflammatory bowel disease in IL-10- and T cell-deficient mice. *Am J Physiol Gastrointest Liver Physiol* 281:G764–78.
  36. Kühn R, Löhler J, Rennick D, Rajewsky K, Müller W. 1993. Interleukin-10-deficient mice develop chronic enterocolitis. *Cell* 75:263–274.
  37. Kennedy RJ, Hoper M, Deodhar K, Erwin PJ, Kirk SJ, Gardiner KR. 2000. Interleukin 10-deficient colitis: new similarities to human inflammatory bowel disease. *Br J Surg* 87:1346–1351.
  38. Rennick DM, Fort MM. 2000. XII. IL-10-deficient (IL-10<sup>-/-</sup>) mice and intestinal inflammation. *Am J Physiol Gastrointest Liver Physiol* 278:G829–G833.
  39. Mähler M, Leiter EH. 2002. Genetic and environmental context determines the course of colitis developing in IL-10-deficient mice. *Inflamm Bowel Dis* 8:347–355.
  40. Chassaing B, Srinivasan G, Delgado MA, Young AN, Gewirtz AT, Vijay-Kumar M. 2012. Fecal Lipocalin 2, a Sensitive and Broadly Dynamic Non-Invasive Biomarker for Intestinal Inflammation. *PLoS One* 7:e44328.
  41. Nowicki D, Maciąg-Dorszyńska M, Bogucka K, Szalewska-Pałasz A, Herman-Antosiewicz A. 2019. Various modes of action of dietary phytochemicals, sulforaphane and phenethyl isothiocyanate, on pathogenic bacteria. *Sci Rep* 9:13677.
  42. Fahey JW, Haristoy X, Dolan PM, Kensler TW, Scholtus I, Stephenson KK, Talalay P,

- Lozniewski A. 2002. Sulforaphane inhibits extracellular, intracellular, and antibiotic-resistant strains of *Helicobacter pylori* and prevents benzo[a]pyrene-induced stomach tumors. *Proc Natl Acad Sci U S A* 99:7610–7615.
43. Sikorska-Zimny K, Beneduce L. 2021. The Metabolism of Glucosinolates by Gut Microbiota. *Nutrients* 13:2750.
44. Okayasu I, Hatakeyama S, Yamada M, Ohkusa T, Inagaki Y, Nakaya R. 1990. A novel method in the induction of reliable experimental acute and chronic ulcerative colitis in mice. *Gastroenterology* 98:694–702.
45. Poritz LS, Garver KI, Green C, Fitzpatrick L, Ruggiero F, Koltun WA. 2007. Loss of the tight junction protein ZO-1 in dextran sulfate sodium induced colitis. *J Surg Res* 140:12–19.
46. Chassaing B, Aitken JD, Malleshappa M, Vijay-Kumar M. 2014. Dextran sulfate sodium (DSS)-induced colitis in mice. *Curr Protoc Immunol* 104:15.25.1–15.25.14.
47. Araki A, Kanai T, Ishikura T, Makita S, Uraushihara K, Iiyama R, Totsuka T, Takeda K, Akira S, Watanabe M. 2005. MyD88-deficient mice develop severe intestinal inflammation in dextran sodium sulfate colitis. *J Gastroenterol* 40:16–23.
48. Dieleman LA, Ridwan BU, Tennyson GS, Beagley KW, Bucy RP, Elson CO. 1994. Dextran sulfate sodium-induced colitis occurs in severe combined immunodeficient mice. *Gastroenterology* 107:1643–1652.
49. Bhattacharyya S, Dudeja PK, Tobacman JK. 2009. ROS, Hsp27, and IKKbeta mediate dextran sodium sulfate (DSS) activation of I $\kappa$ B $\alpha$ , NF $\kappa$ B, and IL-8. *Inflamm Bowel Dis* 15:673–683.
50. Yang Y, Jia H, Lyu W, Furukawa K, Li X, Hasebe Y, Kato H. 2022. Dietary Eggshell

Membrane Powder Improves Survival Rate and Ameliorates Gut Dysbiosis in Interleukin-10 Knockout Mice. *Front Nutr* 9:895665.

51. Wang D, Jin H, Sheng J, Cheng L, Lin Q, Lazerev M, Jin P, Li X. 2022. A high salt diet protects interleukin 10-deficient mice against chronic colitis by improving the mucosal barrier function. *Mol Immunol* 150:39–46.
52. Zhang Z, Hyun JE, Thiesen A, Park H, Hotte N, Watanabe H, Higashiyama T, Madsen KL. 2020. Sex-Specific Differences in the Gut Microbiome in Response to Dietary Fiber Supplementation in IL-10-Deficient Mice. *Nutrients* 12:2088.
53. Kondo H, Abe I, Gotoh K, Fukui A, Takanari H, Ishii Y, Ikebe Y, Kira S, Oniki T, Saito S, Aoki K, Tanino T, Mitarai K, Kawano K, Miyoshi M, Fujinami M, Yoshimura S, Ayabe R, Okada N, Nagano Y, Akioka H, Shinohara T, Akiyoshi K, Masaki T, Teshima Y, Yufu K, Nakagawa M, Takahashi N. 2018. Interleukin 10 Treatment Ameliorates High-Fat Diet-Induced Inflammatory Atrial Remodeling and Fibrillation. *Circ Arrhythm Electrophysiol* 11:e006040.
54. Kowalski GM, Nicholls HT, Risis S, Watson NK, Kanellakis P, Bruce CR, Bobik A, Lancaster GI, Febbraio MA. 2011. Deficiency of haematopoietic-cell-derived IL-10 does not exacerbate high-fat-diet-induced inflammation or insulin resistance in mice. *Diabetologia* 54:888–899.
55. Knoop KA, McDonald KG, Coughlin PE, Kulkarni DH, Gustafsson JK, Rusconi B, John V, Ndao IM, Beigelman A, Good M, Warner BB, Elson CO, Hsieh C-S, Hogan SP, Tarr PI, Newberry RD. 2020. Synchronization of mothers and offspring promotes tolerance and limits allergy. *JCI Insight* 5:e137943.
56. Schloss PD, Schubert AM, Zackular JP, Iverson KD, Young VB, Petrosino JF. 2012.

- Stabilization of the murine gut microbiome following weaning. *Gut Microbes* 3:383–393.
57. Delage C, Taib T, Mamma C, Lerouet D, Besson VC. 2021. Traumatic Brain Injury: An Age-Dependent View of Post-Traumatic Neuroinflammation and Its Treatment. *Pharmaceutics* 13:1624.
58. Bäckhed F, Roswall J, Peng Y, Feng Q, Jia H, Kovatcheva-Datchary P, Li Y, Xia Y, Xie H, Zhong H, Khan MT, Zhang J, Li J, Xiao L, Al-Aama J, Zhang D, Lee YS, Kotowska D, Colding C, Tremaroli V, Yin Y, Bergman S, Xu X, Madsen L, Kristiansen K, Dahlgren J, Wang J. 2015. Dynamics and Stabilization of the Human Gut Microbiome during the First Year of Life. *Cell Host Microbe* 17:852.
59. Faith JJ, Guruge JL, Charbonneau M, Subramanian S, Seedorf H, Goodman AL, Clemente JC, Knight R, Heath AC, Leibel RL, Rosenbaum M, Gordon JI. 2013. The Long-Term Stability of the Human Gut Microbiota. *Science* 341:1237439.
60. Berding K, Holscher HD, Arthur AE, Donovan SM. 2018. Fecal microbiome composition and stability in 4- to 8-year old children is associated with dietary patterns and nutrient intake. *J Nutr Biochem* 56:165–174.
61. Kemp KM, Colson J, Lorenz RG, Maynard CL, Pollock JS. 2021. Early life stress in mice alters gut microbiota independent of maternal microbiota inheritance. *Am J Physiol Regul Integr Comp Physiol* 320:R663–R674.
62. Lynn MA, Eden G, Ryan FJ, Bensalem J, Wang X, Blake SJ, Choo JM, Chern YT, Sribnaia A, James J, Benson SC, Sandeman L, Xie J, Hassiotis S, Sun EW, Martin AM, Keller MD, Keating DJ, Sargeant TJ, Proud CG, Wesselingh SL, Rogers GB, Lynn DJ. 2021. The composition of the gut microbiota following early-life antibiotic exposure affects host health and longevity in later life. *Cell Rep* 36:109564.

63. Li X, Ren Y, Zhang J, Ouyang C, Wang C, Lu F, Yin Y. 2022. Development of Early-Life Gastrointestinal Microbiota in the Presence of Antibiotics Alters the Severity of Acute DSS-Induced Colitis in Mice. *Microbiol Spectr* 10:e0269221.
64. Knoch B, Nones K, Barnett MPG, McNabb WC, Roy NC. 2010. Diversity of caecal bacteria is altered in interleukin-10 gene-deficient mice before and after colitis onset and when fed polyunsaturated fatty acids. *Microbiology* 156:3306–3316.
65. Overstreet A-MC, Ramer-Tait AE, Suchodolski JS, Hostetter JM, Wang C, Jergens AE, Phillips GJ, Wannemuehler MJ. 2020. Temporal Dynamics of Chronic Inflammation on the Cecal Microbiota in IL-10<sup>-/-</sup> Mice. *Front Immunol* 11:585431.
66. Le Chatelier E, Nielsen T, Qin J, Prifti E, Hildebrand F, Falony G, Almeida M, Arumugam M, Batto J-M, Kennedy S, Leonard P, Li J, Burgdorf K, Grarup N, Jørgensen T, Brandslund I, Nielsen HB, Juncker AS, Bertalan M, Levenez F, Pons N, Rasmussen S, Sunagawa S, Tap J, Tims S, Zoetendal EG, Brunak S, Clément K, Doré J, Kleerebezem M, Kristiansen K, Renault P, Sicheritz-Ponten T, de Vos WM, Zucker J-D, Raes J, Hansen T, Bork P, Wang J, Ehrlich SD, Pedersen O. 2013. Richness of human gut microbiome correlates with metabolic markers. *Nature* 500:541–546.
67. Park JH, Kwon JG, Kim SJ, Song DK, Lee SG, Kim ES, Cho KB, Jang BI, Kim DH, Sin J-I, Kim TW, Song IH, Park KS. 2015. Alterations of colonic contractility in an interleukin-10 knockout mouse model of inflammatory bowel disease. *J Neurogastroenterol Motil* 21:51–61.
68. Wright EK, Kamm MA, Teo SM, Inouye M, Wagner J, Kirkwood CD. 2015. Recent advances in characterizing the gastrointestinal microbiome in Crohn's disease: a systematic review. *Inflamm Bowel Dis* 21:1219–1228.

69. Cohen SL, Moore AM, Ward WE. 2004. Interleukin-10 knockout mouse: a model for studying bone metabolism during intestinal inflammation. *Inflamm Bowel Dis* 10:557–563.
70. Pickard JM, Zeng MY, Caruso R, Núñez G. 2017. Gut microbiota: Role in pathogen colonization, immune responses, and inflammatory disease. *Immunol Rev* 279:70–89.
71. Baumgart DC, Sandborn WJ. 2012. Crohn’s disease. *Lancet* 380:1590–1605.
72. Chiodini RJ, Dowd SE, Chamberlin WM, Galandiuk S, Davis B, Glassing A. 2015. Microbial Population Differentials between Mucosal and Submucosal Intestinal Tissues in Advanced Crohn’s Disease of the Ileum. *PLoS One* 10:e0134382.
73. Hedin CR, McCarthy NE, Louis P, Farquharson FM, McCartney S, Taylor K, Prescott NJ, Murrells T, Stagg AJ, Whelan K, Lindsay JO. 2014. Altered intestinal microbiota and blood T cell phenotype are shared by patients with Crohn’s disease and their unaffected siblings. *Gut* 63:1578–1586.
74. Sokol H, Pigneur B, Watterlot L, Lakhdari O, Bermúdez-Humarán LG, Gratadoux J-J, Blugeon S, Bridonneau C, Furet J-P, Corthier G, Grangette C, Vasquez N, Pochart P, Trugnan G, Thomas G, Blottière HM, Doré J, Marteau P, Seksik P, Langella P. 2008. *Faecalibacterium prausnitzii* is an anti-inflammatory commensal bacterium identified by gut microbiota analysis of Crohn disease patients. *Proc Natl Acad Sci U S A* 105:16731–16736.
75. Ridlon JM, Devendran S, Alves JM, Doden H, Wolf PG, Pereira GV, Ly L, Volland A, Takei H, Nittono H, Murai T, Kurosawa T, Chlipala GE, Green SJ, Hernandez AG, Fields CJ, Wright CL, Kakiyama G, Cann I, Kashyap P, McCracken V, Gaskins HR. 2020. The “in vivo lifestyle” of bile acid 7 $\alpha$ -dehydroxylating bacteria: comparative genomics, metatranscriptomic, and bile acid metabolomics analysis of a defined microbial community in gnotobiotic mice. *Gut Microbes* 11:381–404.

76. Sonnenburg JL, Xu J, Leip DD, Chen C-H, Westover BP, Weatherford J, Buhler JD, Gordon JI. 2005. Glycan foraging in vivo by an intestine-adapted bacterial symbiont. *Science* 307:1955–1959.
77. Chichlowski M, Sharp JM, Vanderford DA, Myles MH, Hale LP. 2008. *Helicobacter typhlonius* and *Helicobacter rodentium* differentially affect the severity of colon inflammation and inflammation-associated neoplasia in IL10-deficient mice. *Comp Med* 58:534–541.
78. Abukhabta S, Khalil Ghawi S, Karatzas KA, Charalampopoulos D, McDougall G, Allwood JW, Verrall S, Lavery S, Latimer C, Pourshahidi LK, Lawther R, O'Connor G, Rowland I, Gill CIR. 2021. Sulforaphane-enriched extracts from glucoraphanin-rich broccoli exert antimicrobial activity against gut pathogens in vitro and innovative cooking methods increase in vivo intestinal delivery of sulforaphane. *Eur J Nutr* 60:1263–1276.
79. Wang R, Halimulati M, Huang X, Ma Y, Li L, Zhang Z. 2022. Sulforaphane-driven reprogramming of gut microbiome and metabolome ameliorates the progression of hyperuricemia. *J Advert Res* In Press.
80. Liou CS, Sirk SJ, Diaz CAC, Klein AP, Fischer CR, Higginbottom SK, Erez A, Donia MS, Sonnenburg JL, Sattely ES. 2020. A Metabolic Pathway for Activation of Dietary Glucosinolates by a Human Gut Symbiont. *Cell* 180:717–728.e19.
81. Luang-In V, Albaser AA, Nueno-Palop C, Bennett MH, Narbad A, Rossiter JT. 2016. Glucosinolate and Desulfo-glucosinolate Metabolism by a Selection of Human Gut Bacteria. *Curr Microbiol* 73:442–451.
82. Laiz L, Miller AZ, Jurado V, Akatova E, Sanchez-Moral S, Gonzalez JM, Dionísio A, Macedo MF, Saiz-Jimenez C. 2009. Isolation of five *Rubrobacter* strains from biodeteriorated monuments. *Naturwissenschaften* 96:71–79.

83. Narbad A, Rossiter JT. 2018. Gut Glucosinolate Metabolism and Isothiocyanate Production. *Mol Nutr Food Res* 62:e1700991.
84. Büchler G, Wos-Oxley ML, Smoczek A, Zschemisch N-H, Neumann D, Pieper DH, Hedrich HJ, Bleich A. 2012. Strain-specific colitis susceptibility in IL10-deficient mice depends on complex gut microbiota-host interactions. *Inflamm Bowel Dis* 18:943–954.
85. Tropini C, Earle KA, Huang KC, Sonnenburg JL. 2017. The Gut Microbiome: Connecting Spatial Organization to Function. *Cell Host Microbe* 21:433–442.
86. Kadriu H, Yeoman C. 2022. The Unseen Minority: Biogeographical Investigations of the Ruminant Gastrointestinal Microbiome Highlight the Importance of Frequently Ignored Anatomical Regions, p. 179–191. *In* Kogut, MH, Zhang, G (eds.), *Gut Microbiota, Immunity, and Health in Production Animals*. Springer International Publishing, Cham, Switzerland.
87. Suzuki TA, Nachman MW. 2016. Spatial Heterogeneity of Gut Microbial Composition along the Gastrointestinal Tract in Natural Populations of House Mice. *PLoS One* 11:e0163720.
88. Yeoman CJ, Ishaq SL, Bichi E, Olivo SK, Lowe J, Aldridge BM. 2018. Biogeographical differences in the influence of maternal microbial sources on the early successional development of the bovine neonatal gastrointestinal tract. *Sci Rep* 8:3197.
89. Hildebrand F, Nguyen TLA, Brinkman B, Yunta RG, Cauwe B, Vandenabeele P, Liston A, Raes J. 2013. Inflammation-associated enterotypes, host genotype, cage and inter-individual effects drive gut microbiota variation in common laboratory mice. *Genome Biol* 14:R4.
90. Kozik AJ, Nakatsu CH, Chun H, Jones-Hall YL. 2019. Comparison of the fecal, cecal, and mucus microbiome in male and female mice after TNBS-induced colitis. *PLoS One* 14:e0225079.

91. Hubbard TD, Murray IA, Nichols RG, Cassel K, Podolsky M, Kuzu G, Tian Y, Smith P, Kennett MJ, Patterson AD, Perdew GH. 2017. Dietary Broccoli Impacts Microbial Community Structure and Attenuates Chemically Induced Colitis in Mice in an Ah receptor dependent manner. *J Funct Foods* 37:685–698.
92. Seifert HA, Gerstner G, Kent G, Vandebark AA, Offner H. 2019. Estrogen-induced compensatory mechanisms protect IL-10-deficient mice from developing EAE. *J Neuroinflammation* 16:195.
93. Bábíčková J, Tóthová L, Lengyelová E, Bartoňová A, Hodosy J, Gardlík R, Celec P. 2015. Sex Differences in Experimentally Induced Colitis in Mice: a Role for Estrogens. *Inflammation* 38:1996–2006.
94. Jašarević E, Howerton CL, Howard CD, Bale TL. 2015. Alterations in the Vaginal Microbiome by Maternal Stress Are Associated With Metabolic Reprogramming of the Offspring Gut and Brain. *Endocrinology* 156:3265–3276.
95. Park KT, Ehrlich OG, Allen JI, Meadows P, Szigethy EM, Henrichsen K, Kim SC, Lawton RC, Murphy SM, Regueiro M, Rubin DT, Engel-Nitz NM, Heller CA. 2020. The Cost of Inflammatory Bowel Disease: An Initiative From the Crohn's & Colitis Foundation. *Inflamm Bowel Dis* 26:1–10.
96. Singh S, Qian AS, Nguyen NH, Ho SKM, Luo J, Jairath V, Sandborn WJ, Ma C. 2022. Trends in U.S. Health Care Spending on Inflammatory Bowel Diseases, 1996-2016. *Inflamm Bowel Dis* 28:364–372.
97. Peery AF, Crockett SD, Murphy CC, Lund JL, Dellon ES, Williams JL, Jensen ET, Shaheen NJ, Barritt AS, Lieber SR, Kochar B, Barnes EL, Fan YC, Pate V, Galanko J, Baron TH, Sandler RS. 2019. Burden and Cost of Gastrointestinal, Liver, and Pancreatic Diseases in

- the United States: Update 2018. *Gastroenterology* 156:254–272.e11.
98. Li Y, Zhang T, Holman J, McKinstry D, Trindade BC, Mendoza-Castrejon J, Ho S, Sun D, Wells E, Chen G. 2022. A Specific Broccoli Sprout Preparation Reduces Chemically-Induced Colitis Via Gut Microbiota. *Curr Dev Nutr* 6:307–307.
  99. Dieleman LA, Peña AS, Meuwissen SG, van Rees EP. 1997. Role of animal models for the pathogenesis and treatment of inflammatory bowel disease. *Scand J Gastroenterol Suppl* 223:99–104.
  100. Spohn SN, Bianco F, Scott RB, Keenan CM, Linton AA, O'Neill CH, Bonora E, Dickey M, Lavoie B, Wilcox RL, MacNaughton WK, De Giorgio R, Sharkey KA, Mawe GM. 2016. Protective Actions of Epithelial 5-Hydroxytryptamine 4 Receptors in Normal and Inflamed Colon. *Gastroenterology* 151:933–944.e3.
  101. Fadrosch DW, Ma B, Gajer P, Sengamalay N, Ott S, Brotman RM, Ravel J. 2014. An improved dual-indexing approach for multiplexed 16S rRNA gene sequencing on the Illumina MiSeq platform. *Microbiome* 2:6.
  102. Caporaso JG, Lauber CL, Walters WA, Berg-Lyons D, Lozupone CA, Turnbaugh PJ, Fierer N, Knight R. 2011. Global patterns of 16S rRNA diversity at a depth of millions of sequences per sample. *Proc Natl Acad Sci U S A* 108:4516–4522.
  103. 2011. The Earth Microbiome Project. The Earth Microbiome Project. <http://www.earthmicrobiome.org>.
  104. Callahan B. 2022. DADA2: Fast and accurate sample inference from amplicon data with single-nucleotide resolution (1.16). <https://benjjneb.github.io/dada2/tutorial.html>.
  105. RCoreTeam. 2022. R: a language and environment for statistical computing (4.2.2). R

Foundation for Statistical Computing, Vienna, Austria. <https://www.r-project.org/>.

106. Pruesse E, Quast C, Knittel K, Fuchs BM, Ludwig W, Peplies J, Glöckner FO. 2007. SILVA: a comprehensive online resource for quality checked and aligned ribosomal RNA sequence data compatible with ARB. *Nucleic Acids Res* 35:7188–7196.
107. Wickham H, Francois R, Henry L, Müller K. 2015. dplyr: A Grammar of Data Manipulation. R package version 0.4. 3. R Found Stat Comput , Vienna <https://CRAN.R-project.org/package=dplyr>.
108. Ishaq SL. 2017. Phyloseq\_dealing\_with\_neg\_controls\_Ishaq\_example.R. Github. <https://github.com/Suelshaq/Examples-DADA2-Phyloseq>. Retrieved 5 March 2019.
109. McMurdie PJ, Holmes S. 2013. phyloseq: An R Package for Reproducible Interactive Analysis and Graphics of Microbiome Census Data. *PLoS One* 8:e61217.
110. Weiss S, Xu ZZ, Peddada S, Amir A, Bittinger K, Gonzalez A, Lozupone C, Zaneveld JR, Vázquez-Baeza Y, Birmingham A, Hyde ER, Knight R. 2017. Normalization and microbial differential abundance strategies depend upon data characteristics. *Microbiome* 5:27.
111. Cameron ES, Schmidt PJ, Tremblay BJ-M, Emelko MB, Müller KM. 2021. Enhancing diversity analysis by repeatedly rarefying next generation sequencing data describing microbial communities. *Sci Rep* 11:22302.
112. Bates D, Mächler M, Zurich E, Bolker BM, Walker SC. 2015. Fitting Linear Mixed-Effects Models Using lme4. *Journal of Statistical Software, Articles* 67:1–48.
113. Oksanen J, Guillaume Blanchet F, Friendly M, Kindt R, Legendre P, McGlinn D, Minchin PR, O'Hara RB, Simpson GL, Solymos P, Stevens MHH, Szoecs E, Wagner H. 2020.

- Vegan: Community Ecology Package (2.5-7). <https://cran.r-project.org/web/packages/vegan/vignettes/diversity-vegan.pdf>.
114. Archer E. 2022. rfpermute: Estimate Permutation p-Values for Random Forest Importance Metrics (2.5.1). <https://github.com/EricArcher/rfPermute>.
115. Wickham H. 2016. ggplot2: Elegant graphics for Data Analysis. Springer Publishing Company, New York. <https://dl.acm.org/citation.cfm?id=1795559>.
116. Kassambara A. 2022. ggpubr: “ggplot2” based publication ready plots (0.1.7). <https://rpkgs.datanovia.com/ggpubr/>.
117. Knights D, Kuczynski J, Charlson ES, Zaneveld J, Mozer MC, Collman RG, Bushman FD, Knight R, Kelley ST. 2011. Bayesian community-wide culture-independent microbial source tracking. *Nat Methods* 8:761–763.
118. Galey M. 2021. Mi-Seq Analysis. GitHub. <https://mgaley-004.github.io/MiSeq-Analysis/Tutorials/SourceSink.html>, <https://github.com/mgaley-004/MiSeq-Analysis>. Retrieved 7 December 2022.